GENERAL TECHNOLOGY CORPORATION

GENERAL TECHNOLOGY CORPORATION

AN INVESTIGATION OF LOADS, STRESS LEVELS, AND FRICTION TORQUES OF TIMER-MECHANISM BEARINGS

BY

MARTIN SENATOR

APPROVED

R. C. Geldmacher

R. C. Geldmacher

Supervising Consultant

Submitted to Frankford Arsenal under Contract No. DA-11-022 AMC-168(A), AMCMS Code 5530.11.55700.08

General Technolocy Corporation

TABLE OF CONTENTS

INTRODUCTION

The purpose of this investigation is to analyze the effects of axial and transverse acceleration on bearings of various shapes which may be suitable for use in spring driven timer mechanisms. The investigation considers the feasibility of each bearing in terms of loads, stress levels, and friction torques and indicates appropriate design and analysis techniques.

The conventional timer consists of a mainspring as an energy source, a speed increasing set of spur gears and pinions on parallel shafts, and an escapement controlled by an oscillating balance wheel. The case of the timer is fastened to the projectile and accelerations are imparted to the gears and shafts through the bearings under investigation. The usual orientation of a timer is with its shafts parallel to the axis of the projectile and with the center of the timer housing on the axis of symmetry.

Timer bearings are ordinarily subjected to two different types of loading. The first, of short duration, results from acceleration while in the gun tube and acts approximately parallel to the axes of the shafts. During this interval the mechanism may not be required to operate, but it must be able to function properly as soon as the axial load drops off. The second type of loading is caused by a radial acceleration of increasing magnitude while the mechanism is in the gun tube and of approximately constant magnitude during the flight of the projectile. The mechanism is required to function properly while under the latter loading.

The main part of this report is divided into four sections.

In the first section bearings which can withstand axial load are analyzed. Ten different combinations of shape and pressure distribution are considered. Since it is likely that the minimum bearing size will be limited by axial load capacity, formulas are derived in each case expressing the required bearing size as a function of its pertinent geometric parameters and the dimensionless axial load.

These expressions can be used in design in two ways. First, if a particular geometry has been decided upon, they can be used to find the minimum bearing size as determined by axial load capacity. Second, they can be used to see the effects of the various geometric parameters upon bearing size as determined by axial load, and so will serve as a guide in choosing the most suitable shape and parameters. Throughout this section typical numerical values of load, material properties, and geometric parameters are used in the formulas developed in order to give a physical idea of typical sizes. Since some of the formulas developed are represented by fairly complicated equations, many of these equations are plotted in order to determine the general trends of the curves and to facilitate comparisons between the cases. Since operation while under axial load may be required, expressions for the friction torque are also developed for each of the ten cases. Again typical numerical values are calculated in order to give an idea of the orders of magnitude of these quantities and to compare the relative merits of the ten cases.

In the second section of this report the bearings of Section I are analyzed under transverse load. Because flat bearings can withstand axial but not transverse load and because under transverse load one normal pressure distribution is much more reasonable than most others, the ten cases of Section I reduce to four distinct cases. They are: spherical bearings (solid and hollow), torroidal bearings, conical bearings, and bearings with latitude circle line contact. In each of these cases formulas for required bearing size as a function of geometric parameters and applied transverse load are derived. Again typical numerical values are calculated and it is found that with the load magnitudes used here as typical, either axial or transverse load capacity may fix the minimum bearing size. The one that controls depends not only upon the ratio of maximum transverse to axial load, but also upon the type of bearing and the values of its geometric parameters. Again these formulas may be used in two ways - for calculating numerical sizes once the geometry has been fixed, and for evaluating the effects of the various geometric parameters. Since operation while under transverse load is a definite requirement, expressions for the friction torque and typical numerical values are calculated in each of the four cases.

Journal bearings are investigated in the third section of this report. These bearings could be used in conjunction with one or two bearings that have axial load capacity. An approximate method is developed for calculating contact stresses in terms of transverse load, bearing size, and meridian radius of curvature. In addition expressions for friction torque are developed. Again typical loading is considered and numerical values are calculated for this loading.

In the fourth section of the report two topics are investigated. They are the estimation of typical loading and the investigation of the feasibility, for this application, of sharp vee-jewel bearings as used in precision instruments and watches.

SECTION I

BEARINGS WITH AXIAL LOAD CAPACITY

There are three classes of bearing of this type. They may be described as bearings with full contact, bearings with thin ring contact and bearings with theoretical line contact. A bearing from each of these classes is sketched in Figures 1 to 3.

A study of Figures 1 and 2 indicates that the surfaces are initially conforming - that is, in the unloaded condition there is theoretical area contact. In addition, in order to get side thrust capability, and so eliminate the main disadvantage of vee jewel bearings, (see SECTION IV), contact occurs at radii that are of the order of magnitude of the shaft radius. This increases the effective friction radius above that of vee jewel bearings and so gives the (unavoidable) penalty of higher friction torque. However we want numerical values of these parameters in order to evaluate an optimum design.

The various shapes will be considered only under axial load in order to determine the required size. Just as for the vee jewel bearing it is likely that the initial axial acceleration will fix the size. Various normal pressure distributions will be considered for each shape. In addition friction torques will be computed to see what would happen if the bearings have to operate during the axial acceleration period. In SECTION II

FIGURE I

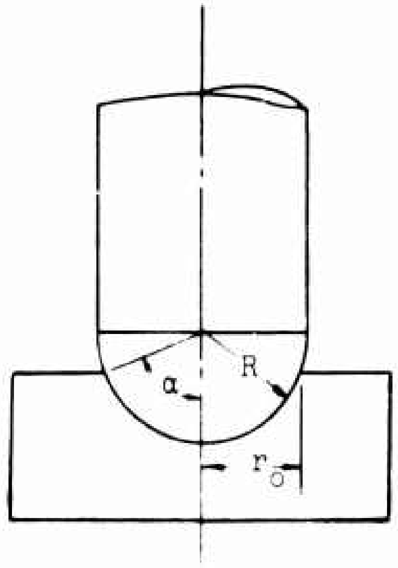

SPHERICAL BEARING, CONVEX SHAFT, AND FULL CONTACT

FIGURE II

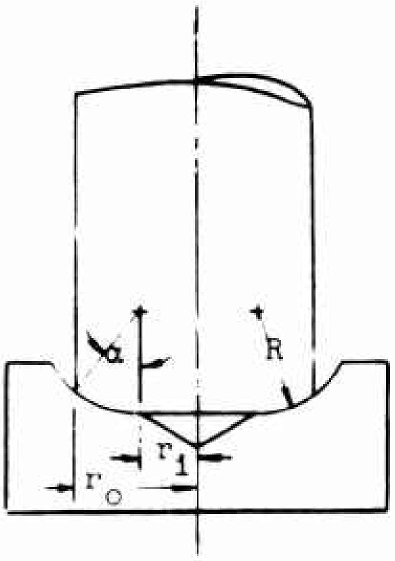

TORROIDAL BEARING, CONVEX SHAFT, AND THIN RING CONTACT

FIGURE III

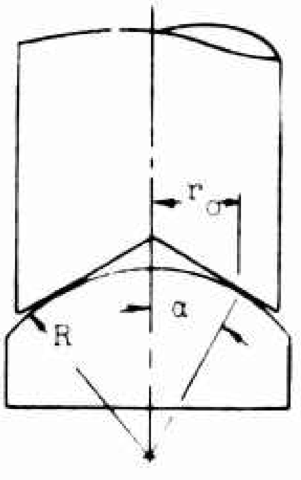

SPHERICAL-CONICAL BEARING, CONCAVE SHAFT, AND THEORETICAL LINE CONTACT these bearings will be considered under transverse loads only; friction torques and bearing contact stresses will be computed in addition to other quantities of interest for a particular bearing.

Case 1 FLAT BEARING - WITH AND WITHOUT A HOLE - UNIFORM PRESSURE DISTRIBUTION - SIZING UNDER AXIAL LOAD

Defining β by

(1) $$\beta = \frac{r_o}{r_i}$$

we get

(2) $$q_o = \frac{P}{\pi(r_o^2 - r_i^2)}$$

and

(3) $$r_o = \left\{\frac{P}{\pi q_o}\left[\frac{1}{1 - (1/\beta)^2}\right]\right\}^{1/2}$$

where r_i and r_o are the inner and outer radii in inches, q_o is the maximum bearing pressure in psi, and P is the axial load in lb. It is readily observed that the minimum size bearing is the one with $\beta = \infty$ (no hole). Thus we define a reference outside radius as

(4) $$(r_o)_{ref} = \left[\frac{P}{\pi q_o}\right]^{1/2}$$

FIGURE IV

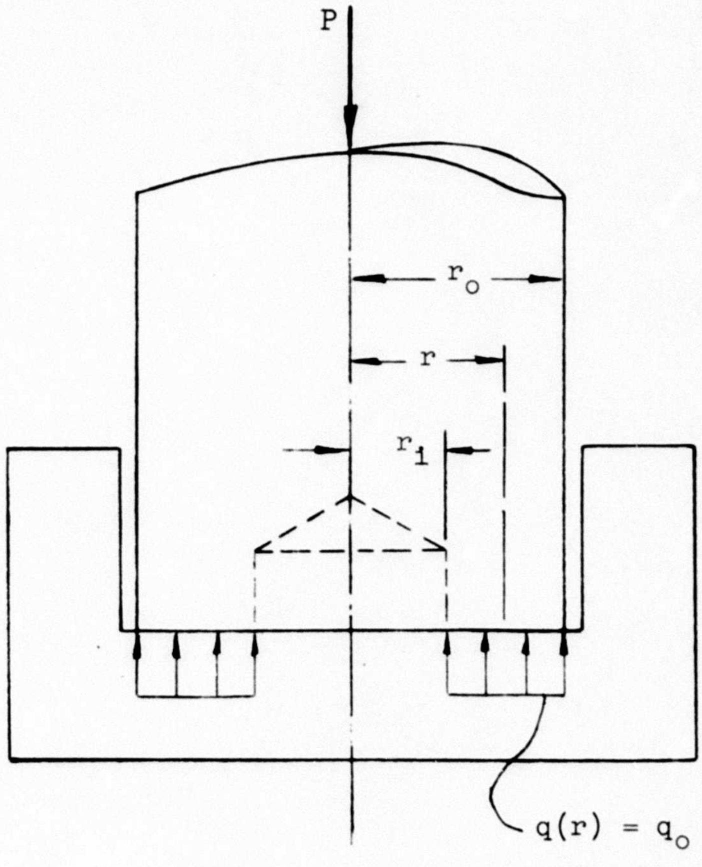

FLAT BEARING

WITH A HOLE

and a dimensionless relative bearing size D as

(5) $$D = \frac{r_o}{(r_o)_{ref}}$$

and get for the solid flat bearing

(6) $$D = 1$$

and for the hollow flat bearing

(7) $$D = \left[\frac{\beta^2}{\beta^2 - 1}\right]^{1/2}$$

The range of β of interest is from $\beta = \infty$ for the solid flat bearing to about $\beta = r_o/(r_o - .1r_o) \approx 1.1$ for relatively thin bearings. (Anything thinner would require excessive tolerances.) The bearing relative size $D = r_o/(r_o)_{ref}$ of equation (7) vs $1/\beta$ is shown in Fig. 5 on Page 10 and tabulated in Table 1 on Page 14. It can be seen that the thinnest section that would be used ($\beta \approx 1.1$) requires about 2.3 times the outside diameter of a no-hole section for the same load P and design normal pressure q_o. In order to investigate typical sizes take $P_{typical} = 15.95$ lb. (See Page 114 of SECTION IV.) It is more difficult to estimate a good design value for q_o. The value chosen should be below $q_o = 285{,}000$ psi (Page 108) since there is area contact in the undeformed position now and the likelihood is high of having much greater than average pressure at

FIGURE V

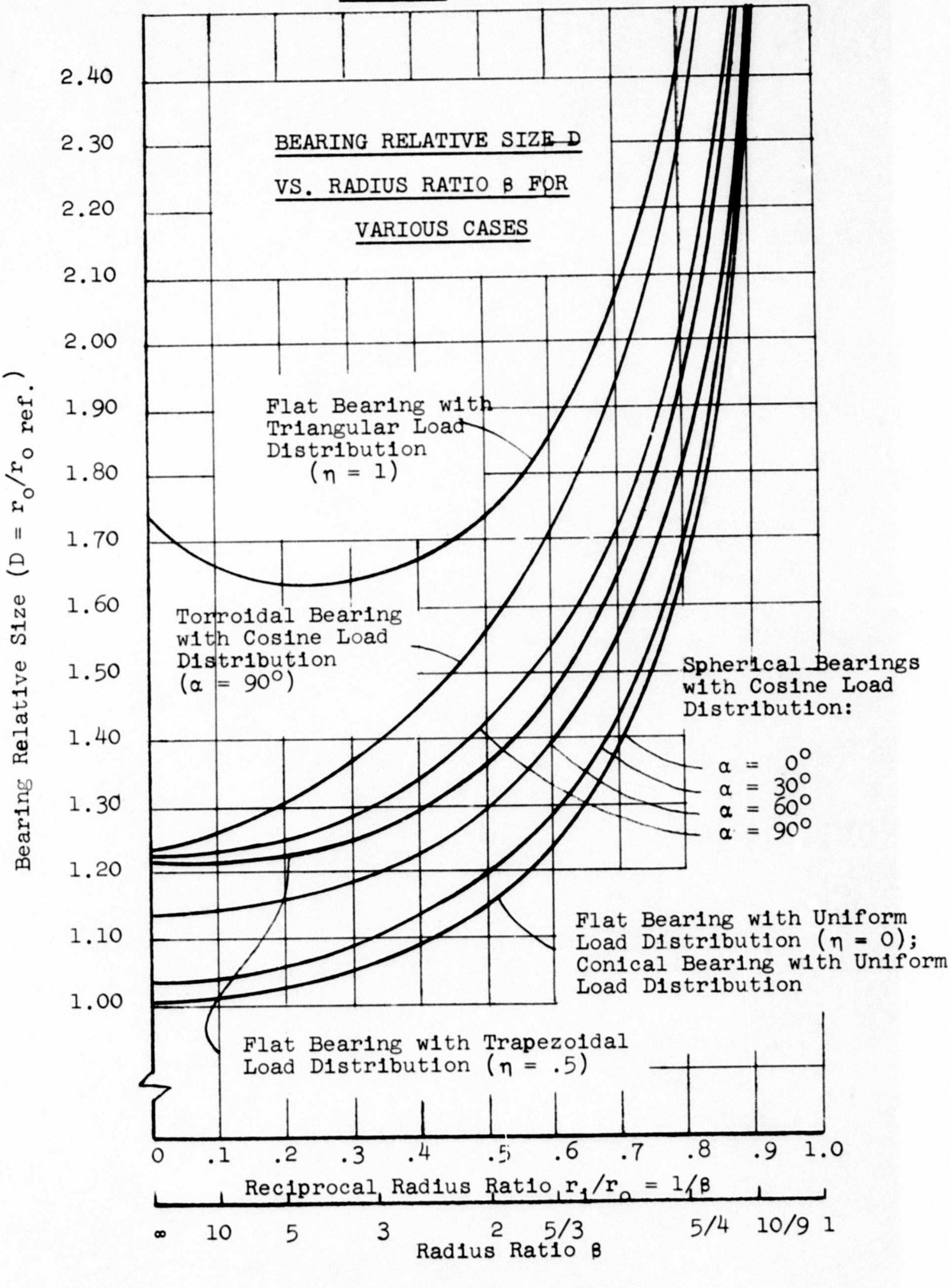
BEARING RELATIVE SIZE D
VS. RADIUS RATIO β FOR
VARIOUS CASES
Bearing Relative Size (D = r_o/r_o ref.)
2.40
2.30
2.20
2.10
2.00
1.90
1.80
1.70
1.60
1.50
1.40
1.30
1.20
1.10
1.00
Flat Bearing with
Triangular Load
Distribution
(η = 1)
Torroidal Bearing
with Cosine Load
Distribution
(α = 90°)
Spherical Bearings
with Cosine Load
Distribution:
α = 0°
α = 30°
α = 60°
α = 90°
Flat Bearing with Uniform
Load Distribution (η = 0);
Conical Bearing with Uniform
Load Distribution
Flat Bearing with Trapezoidal
Load Distribution (η = .5)
0 .1 .2 .3 .4 .5 .6 .7 .8 .9 1.0
Reciprocal Radius Ratio r_i/r_o = 1/β
∞ 10 5 3 2 5/3 5/4 10/9 1
Radius Ratio β

local irregularities. Thus use q_o = 242,000 psi (Page 95) for the relatively thin sections and q_o = 175,000 psi (say) for others.

Then for thin sections

$$(r_o)_{ref \quad min} = \left[\frac{P}{\pi q_o}\right]^{1/2} = \left[\frac{15.95}{(3.14)(242,000)}\right]^{1/2} = .00459 \text{ in.}$$

and for thick sections

$$(r_o)_{ref, \ max} = \left[\frac{P}{\pi q_o}\right]^{1/2} = \left[\frac{15.95}{(3.14)(175,000)}\right]^{1/2} = .00539 \text{ in.}$$

The reference shaft diameters are then

$$(d_o)_{ref, \ min} = .0092 \text{ in. for thin ring contact}$$

and

$$(d_o)_{ref, \ max} = .0108 \text{ in. for larger contact area.}$$

For a ratio of $r_1/r_o = 1/8 \approx .6$, the outside diameter would be $\approx 1.25 \times .0108 \approx .0135$ in. (see Table I), while for $r_1/r_o \approx .9$, the outside diameter would be $\approx 2.3 \times .0092 = .0212$ in. (The higher design stress is used for the relatively thinner contact area.)

Case 2 FLAT BEARING - LINEAR PRESSURE DISTRIBUTIONS-SIZING UNDER AXIAL LOAD

For the relatively thin sections the uniform pressure distribution is quite reasonable. For the thicker ones, in order to prevent corners from digging in, the bearings could be made somewhat as shown in the exaggerated sketch on Page 13, (Figure 6). The small axial clearance shown prevents the outside corners from taking all the load. When the load is applied the two surfaces deform into contact. The resulting normal pressure distribution then drops off with increasing radius.

Thus consider the Trapezoidal Distribution with parameter η shown in Figure 7. Here the normal pressure is given by

$$q(r) = q_o - \eta q_o \frac{r - r_1}{r_o - r_1} \tag{8}$$

When $\eta = o$, this reduces to the uniform distribution; and when $\eta = 1$, it reduces to a triangular distribution. The equation of axial equilibrium gives

$$P = \int_{r = r_1}^{r = r_o} dP = \int_{r_1}^{r_o} (2\pi r dr)(q_o)(1 - \eta \frac{r - r_1}{r_o - r_1}) \tag{9}$$

Integrating, using the definition of bearing relative size D (Equation 5), and simplifying gives

FIGURE VI

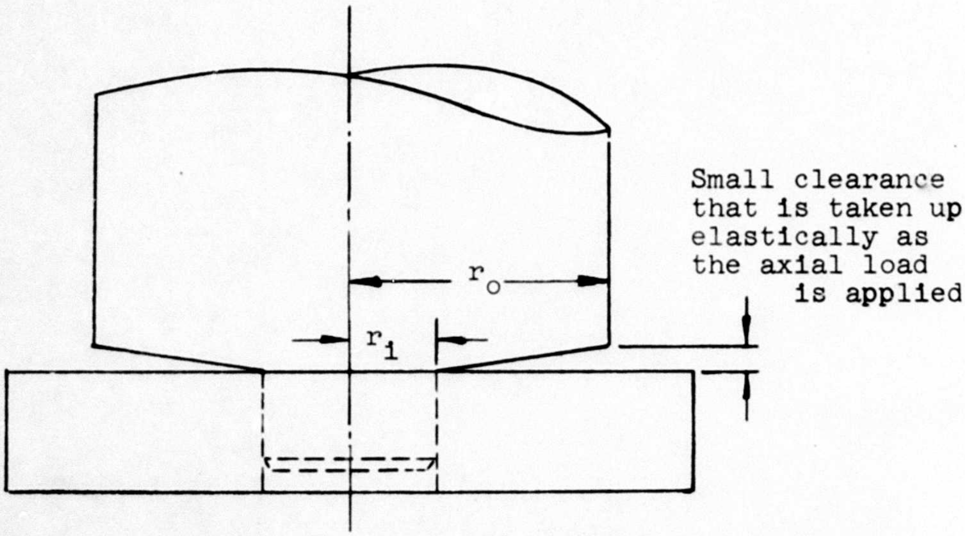

EXAGGERATED VIEW OF A FLAT BEARING

BEFORE THE AXIAL LOAD IS APPLIED

FIGURE VII

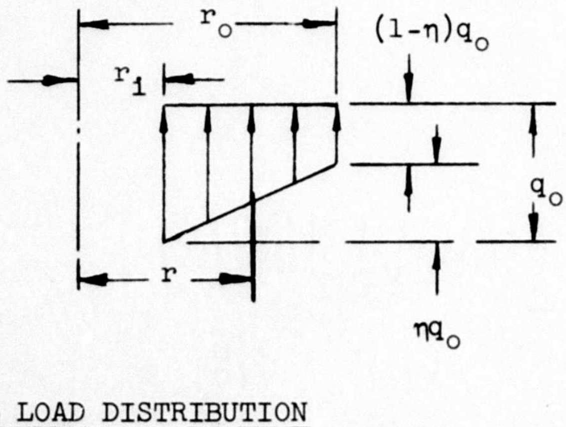

TRAPEZOIDAL LOAD DISTRIBUTION

q(r) FOR A FLAT BEARING

$$D(\beta, \eta) = \left[\frac{\beta^2}{\beta^2 - 1 + (\eta/3)(1 + \beta - 2\beta^2)} \right]^{1/2} \qquad (10)$$

Comparing this to Equation 7, Page 9 shows that it reduces to that equation for $\eta = 0$. The quantity $(1 + \beta - 2\beta^2)$ is zero for $\beta = 1$ (the smallest value of β) and gets smaller (more negative) for increasing β. Thus for any positive η between 0 and 1 the denominator gets less and D increases as expected.

Some tabulated values are given in Table 1 below.

Table 1

BEARING RELATIVE SIZE D AS A FUNCTION OF BEARING RADIUS RATIO β FOR THREE LINEAR LOAD DISTRIBUTIONS

	Uniform	Trapezoidal	Triangular
β	D (η = 0)	D (η = .5)	D (η = 1)
∞	1.000	1.2252	1.732
10	1.005	1.220	1.670
5	1.021	1.225	1.640
3	1.062	1.261	1.642
2	1.153	1.360	1.732
5/3	1.250	1.463	1.848
5/4	1.670	1.940	2.40
10/9	2.295	2.66	3.28

These curves are plotted in Figure 5 on Page 10. For typical flat bearing sizes as determined by axial load we have for $\beta = 1.667$ $(1/\beta = .6)$

Uniform $(\eta = 0)$ $D = 1.25$

$$d_{outside} = D(d_o)_{ref} = .0108\ D = .0135 \text{ in.}$$

Trapezoidal $(\eta = .5)$ $D = 1.46$

$$d_{outside} = D(d_o)_{ref} = .0108\ D = .0158 \text{ in.}$$

Triangular $(\eta = 1)$ $D = 1.85$

$$d_{outside} = D(d_o)_{ref} = .0108\ D = .020 \text{ in.}$$

and for $\beta = 1.11$ $(1/\beta = .9)$

Uniform $(\eta = 0)$ $D = 2.23$

$$d_{outside} = D(d_o)_{ref} = .0092\ D = .0207 \text{ in.}$$

Trapezoidal $(\eta = .5)$ $D = 2.66$

$$d_{outside} = D(d_o)_{ref} = .0092\ D = .0244 \text{ in.}$$

Triangular $(\eta = 1)$ $D = 3.28$

$$d_{outside} = D(d_o)_{ref} = .0092\ D = .0302 \text{ in.}$$

(see Page 11 for $(d_o)_{ref}$)

The trapezoidal distribution with $\eta = .5$ seems most reasonable. Thus to summarize, we have for flat bearings with a trapezoidal distribution with $\eta = .5$ and for P = 15.95 lb. axial load (Page 114), a design bearing stress q_o = 175,000 psi (Page 11), and a radius ratio $1/\beta = r_1/r_o = .6$, an outside diameter of $d_{outside}$ = .0158 in. Also for a thin section flat bearing with the radius ratio now $1/\beta = r_1/r_o = .9$ and the design bearing stress now q_o = 242,000 psi (Page 11), we have $d_{outside}$ = .0244 in. Both of these sizes are reasonable.

Case 3 FULL SPHERICAL BEARING- UNIFORM NORMAL PRESSURE DISTRIBUTION - SIZING UNDER AXIAL LOAD

The radius of the spherical tip is R, r_o is the outside radius of the bearing, α is the total half angle subtended by the bearing, θ is a variable angle, and r is a variable radius as shown in Figure 8. We have

(11) $$\sin\theta = r/R$$

and

(12) $$\sin\alpha = \frac{r_o}{R}$$

FIGURE VIII

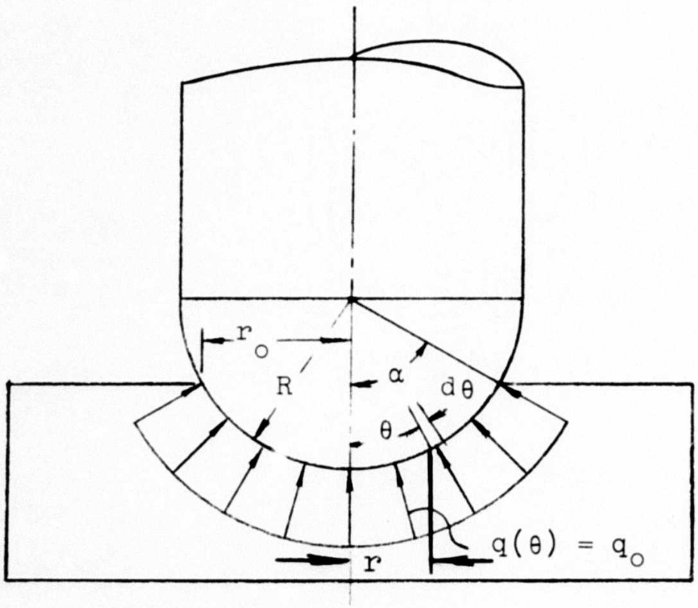

FULL SPHERICAL BEARING WITH

UNIFORM LOAD DISTRIBUTION

FIGURE IX

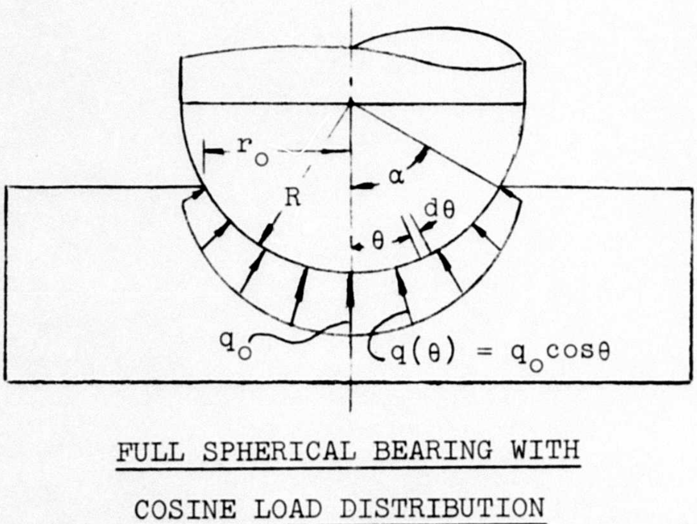

FULL SPHERICAL BEARING WITH

COSINE LOAD DISTRIBUTION

Since the normal pressure distribution is hydrostatic (uniform), its axial resultant equals that of the same uniform pressure distribution over the flat bearing of equal inside and outside diameter. Thus the bearing size is the same as for Case II with $\beta = \infty$ and $\eta = 0$ (Page 14).

Case 4 HOLLOW SPHERICAL BEARING - UNIFORM NORMAL PRESSURE DISTRIBUTION - SIZING UNDER AXIAL LOAD

As noted directly above, the sizes are the same as for the flat bearing with the same radius ratio $\beta = r_o/r_1$ and $\eta = 0$, (Page 14).

Case 5 FULL SPHERICAL BEARING - COSINE NORMAL PRESSURE DISTRIBUTION - SIZING UNDER AXIAL LOAD

Here $q(\theta)$, the normal pressure, is taken as

$$q(\theta) = q_o \cos\theta \qquad (0 \leq \theta \leq \alpha) \tag{13}$$

The equation of axial equilibrium gives (See Figure 9)

$$P = \int dP = \int_{\theta = 0}^{\theta = \alpha} (R d\theta)(2\pi r)(q_o \cos\theta)(\cos\theta) \tag{14}$$

Using the definition of the bearing relative size D, eliminating R and r with equations 11 and 12, and integrating gives

(15) $$D(\alpha) = \left[\frac{3}{2}\right]^{1/2} \left[\frac{\sin\alpha}{(1 - \cos^3\alpha)^{1/2}}\right]$$

As a check, for small values of α this becomes

(16) $$D(\alpha) = \left[\frac{3}{2}\right]^{1/2} \frac{\alpha - \frac{\alpha^3}{6} + \ldots}{\left[1 - (1 - \frac{\alpha^2}{2} + \ldots)^3\right]^{1/2}}$$

$$= \left[\frac{3}{2}\right]^{1/2} \frac{\alpha - \frac{\alpha^3}{6} + \ldots}{\left[\frac{3}{2}\alpha^2 - \ldots\right]^{1/2}}$$

which has the limiting value one. Since small α means essentially a solid flat bearing with a uniform load distribution, this checks with the results for a flat bearing with $\theta = \infty$ and $\eta = 0$.

A tabulation of this function and a plot of it are given in Table 2 and Figure 10.

Table 2

BEARING RELATIVE SIZE D VS BEARING ANGLE α FOR FULL SPHERICAL BEARINGS WITH A COSINE LOAD DISTRIBUTION

α	$D(\alpha)$
0	1.000
10°	1.002
20°	1.022
30°	1.036
45°	1.079
60°	1.136
90°	1.225

Since practical bearing angles would have 90° as an upper limit and since the cosine distribution is reasonable, a solid spherical (conforming) bearing is at most 1.225 times the diameter of a solid flat bearing for the same axial load and design stress.

FIGURE X

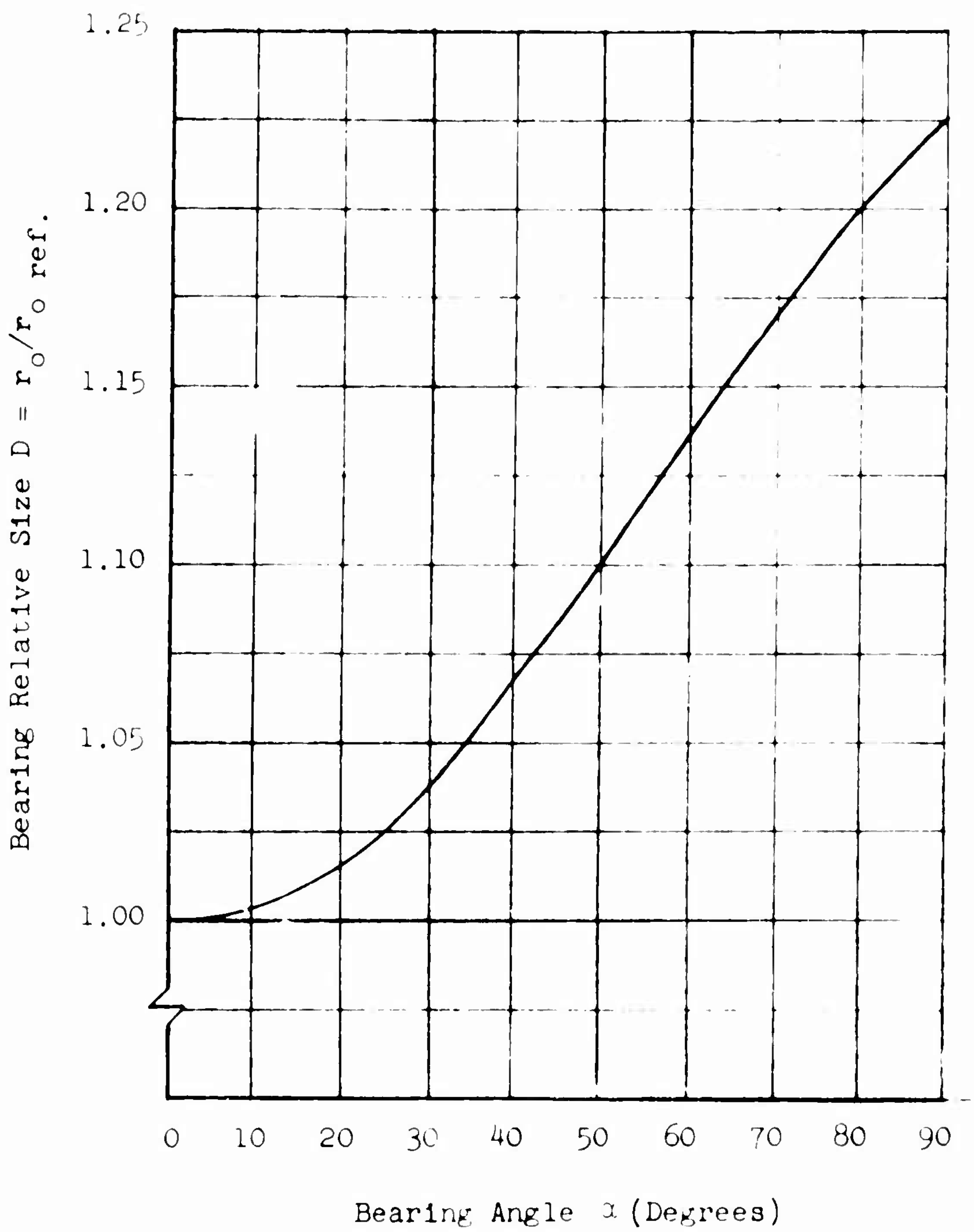

BEARING RELATIVE SIZE VS. BEARING ANGLE FOR A FULL SPHERICAL BEARING WITH A COSINE NORMAL PRESSURE DISTRIBUTION

Case 6 HOLLOW SPHERICAL BEARING WITH COSINE NORMAL PRESSURE DISTRIBUTION - SIZING UNDER AXIAL LOAD

Equation 14 holds with the lower limit replaced by α_1 and with q_o replaced by $q_o/\cos\alpha_1$, where r_1 and α_1 are related by

(17) $$\sin \alpha_1 = \frac{r_1}{R}$$

The integrated equation becomes

(18) $$D(\alpha,\alpha_1) = \left[\frac{3}{2}\right]^{1/2} \frac{\sin\alpha \left[\cos\alpha_1\right]^{1/2}}{\left[\cos^3\alpha_1 - \cos^3\alpha\right]^{1/2}}$$

where α_1 and the radius ratio ρ are related by

(19) $$\rho = \frac{\sin\alpha}{\sin\alpha_1}$$

Some values of D vs. ρ and α are tabulated below in Table 3 and plotted in Figure 5.

Table 3

BEARING RELATIVE SIZE D VS RADIUS RATIO a FOR FOUR BEARING ANGLES α

$\alpha = 0^\circ$ (This corresponds to the flat bearing with a uniform distribution of pressure)

a	α_1	$D(\alpha, \alpha_1) = D(\alpha, a)$
∞	0	1.000 (Solid flat brg) Page 14
10	0	1.005
5	0	1.021
3	0	1.062
2	0	1.153
5/3	0	1.250
5/4	0	1.670
10/9	0	2.295

$\alpha = 30^\circ$

β	α_1	$D(\alpha, \alpha_1) = D(\alpha, \beta)$
∞	0.00°	1.036 (Solid sph. brg.) Page 20
10	2.86°	1.039
5	5.73°	1.056
3	9.60°	1.101
2	14.48°	1.186
5/3	17.47°	1.283
5/4	23.60°	1.688
10/9	26.75°	2.29

$\alpha = 60^\circ$

β	α_1	$D(\alpha_1\ \alpha_1) = D(\alpha_1 \beta)$
∞	0.00°	1.136 (Solid sph. brg.) Page 20
10	4.96°	1.140
5	9.99°	1.159
3	16.73°	1.198
2	25.7°	1.293
5/3	31.3°	1.390
5/4	43.7°	1.808
10/9	51.2°	2.40

$\alpha = 90^\circ$

β	α_1	$D(\alpha_1\ \gamma_1) = D(\alpha_1\ \beta)$
∞	0.00°	1.225 (Solid sph. brg) Page 20
10	5.73°	1.232
5	11.54°	1.252
3	19.48°	1.300
2	30.00°	1.429
5/3	36.8°	1.532
5/4	53.2°	2.04
10/9	64.2°	2.82

Case 7 HOLLOW TORROIDAL BEARING - UNIFORM NORMAL PRESSURE DISTRIBUTION - SIZING UNDER AXIAL LOAD

For this case

(20) $$q(\theta) = q_o$$

(21) $$\frac{r - r_1}{R} = \sin\theta$$

(22) $$\frac{r_o - r_1}{R} = \sin\alpha$$

and

(23) $$P = \int_{\theta = 0}^{\theta = \alpha} dP(\theta) = \int_0^\alpha (q_o)(2\pi r)(R d\theta)(\cos\theta)$$

FIGURE XI

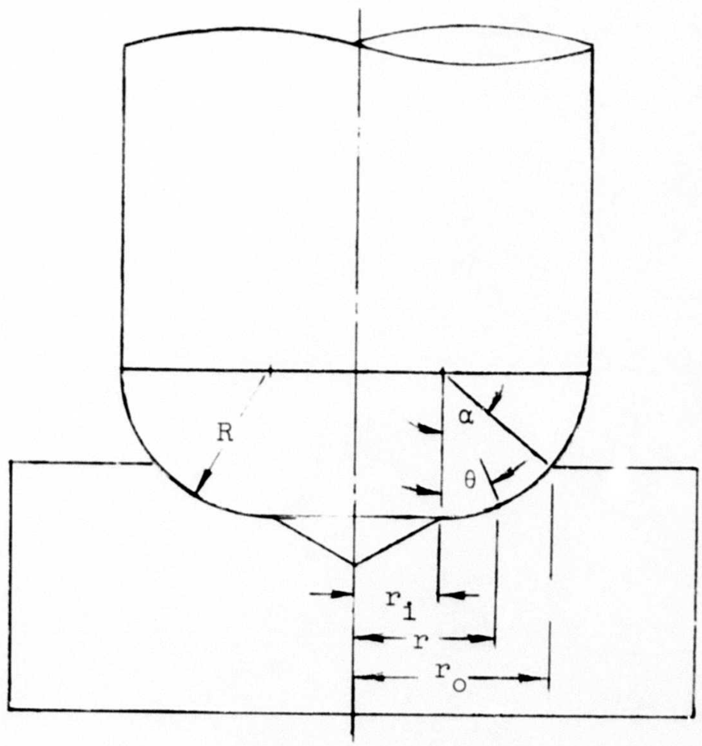

TORROIDAL BEARING

Combining and carrying out the integration gives the same result as for the flat bearing with a uniform load and the same inside and outside radii, namely

$$D = \left[\frac{\beta^2}{\beta^2 - 1}\right]^{1/2} \qquad \text{(See Equation 7)}$$

(See cases 3 and 4 for similar results)

Case 8 HOLLOW TORROIDAL BEARING - COSINE NORMAL PRESSURE DISTRIBUTION - SIZING UNDER AXIAL LOAD

Here instead of Eqs. 20 and 23 we have

(25) $$q(\theta) = q_o \cos\theta$$

and

(26) $$P = \int_{\theta=0}^{\theta=\alpha} dP_{axial}(\theta) = \int_0^{\alpha} (q_o \cos\theta)(2\pi r)(R d\theta)(\cos\theta)$$

respectively. Integrating and using the definitions of D and β (Eqs. 5 and 1) gives

(27) $$D(\beta,\alpha) = \left[\frac{\beta^2}{(\beta-1)^2 \left(\frac{2}{3}\right)\left(\frac{1-\cos^3\alpha}{\sin^2\alpha}\right) + (\beta-1)\left(\frac{\alpha}{\sin\alpha} + \frac{\sin 2\alpha}{2\sin\alpha}\right)}\right]^{1/2}$$

As α approaches zero, this approaches $\left[\frac{\beta^2}{\beta^2 - 1}\right]^{1/2}$ as it should.

Some results are given below in Table 4 for $\alpha = 90^\circ$.

Table 4

BEARING SIZE D VS BEARING RADIUS RATIO β FOR A TORROIDAL BEARING WITH A COSINE LOAD DISTRIBUTION AND AN ANGLE α OF 90°

$\alpha = 90^\circ$	β	$D(\beta, 90^\circ)$	
	∞	1.225	(See P. 25 for a solid sph. brg. with a cos. dist.)
	10	1.258	
	5	1.304	
	3	1.387	
	2	1.548	
	5/3	1.695	
	5/4	2.31	
	10/9	3.22	

Case 9 HOLLOW CONICAL BEARING - UNIFORM NORMAL PRESSURE DISTRIBUTION - SIZING UNDER AXIAL LOAD

The same results hold as for the flat bearing with a uniform normal pressure distribution. This is included here just to get a case number and a sketch for reference (See Figure 12).

FIGURE XII

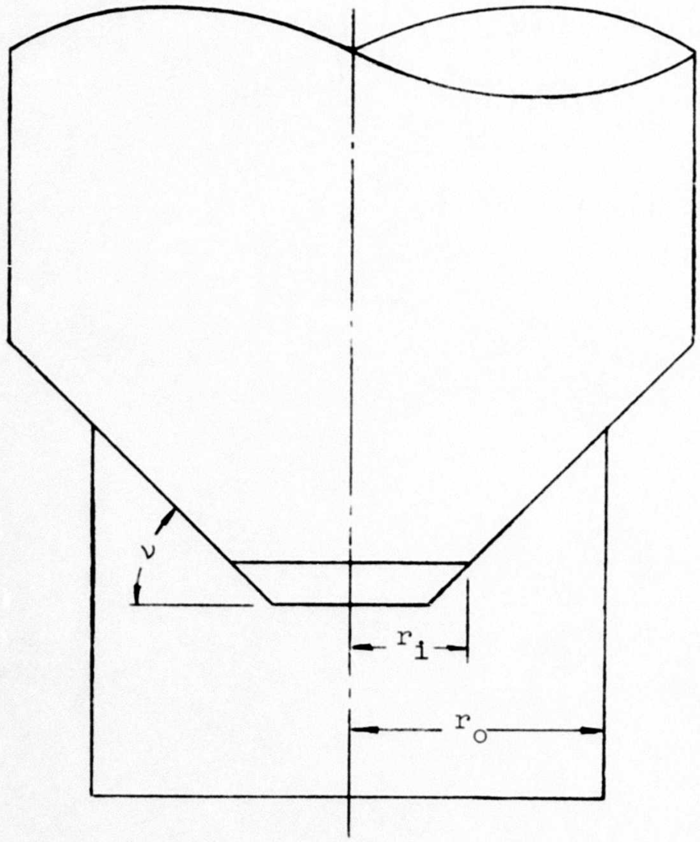

HOLLOW CONICAL BEARING

Case 10 BEARING WITH THEORETICAL LINE CONTACT - SIZING UNDER AXIAL LOAD

In the sketch, (Figure 13), the bearing has theoretical line contact at a radius r_o. The normal to the surfaces makes an angle ν with the shaft axis. R_1 is the meridian radius of curvature of the shaft, positive if the shaft is convex, as shown. R_2 is the meridian radius of curvature of the bearing, also positive if the bearing is convex, as shown. The other two principal radii of curvature, R_1' and R_2', are always equal and opposite to each other in sign as shown, as the mating surfaces co form in one direction. R_1 and R_2 may each be infinite or negative, but neither may be zero. The quantity R_o defined by (See Eqs. 126 or 130)

$$(126) \qquad \frac{1}{R_o} = \frac{1}{R_1} + \frac{1}{R_2}$$

must be positive in order to have theoretical line contact ($R_o = +\infty$ means the most conformity, $R_o = +\varepsilon > o$ means the least conformity). In terms of the notation of equations (119) and (121) we have

$$(119) \qquad A + B = \frac{1}{2} \left(\frac{1}{R_1} + \frac{1}{R_1'} + \frac{1}{R_2} + \frac{1}{R_2'} \right) = \frac{1}{2R_o}$$

FIGURE XIII

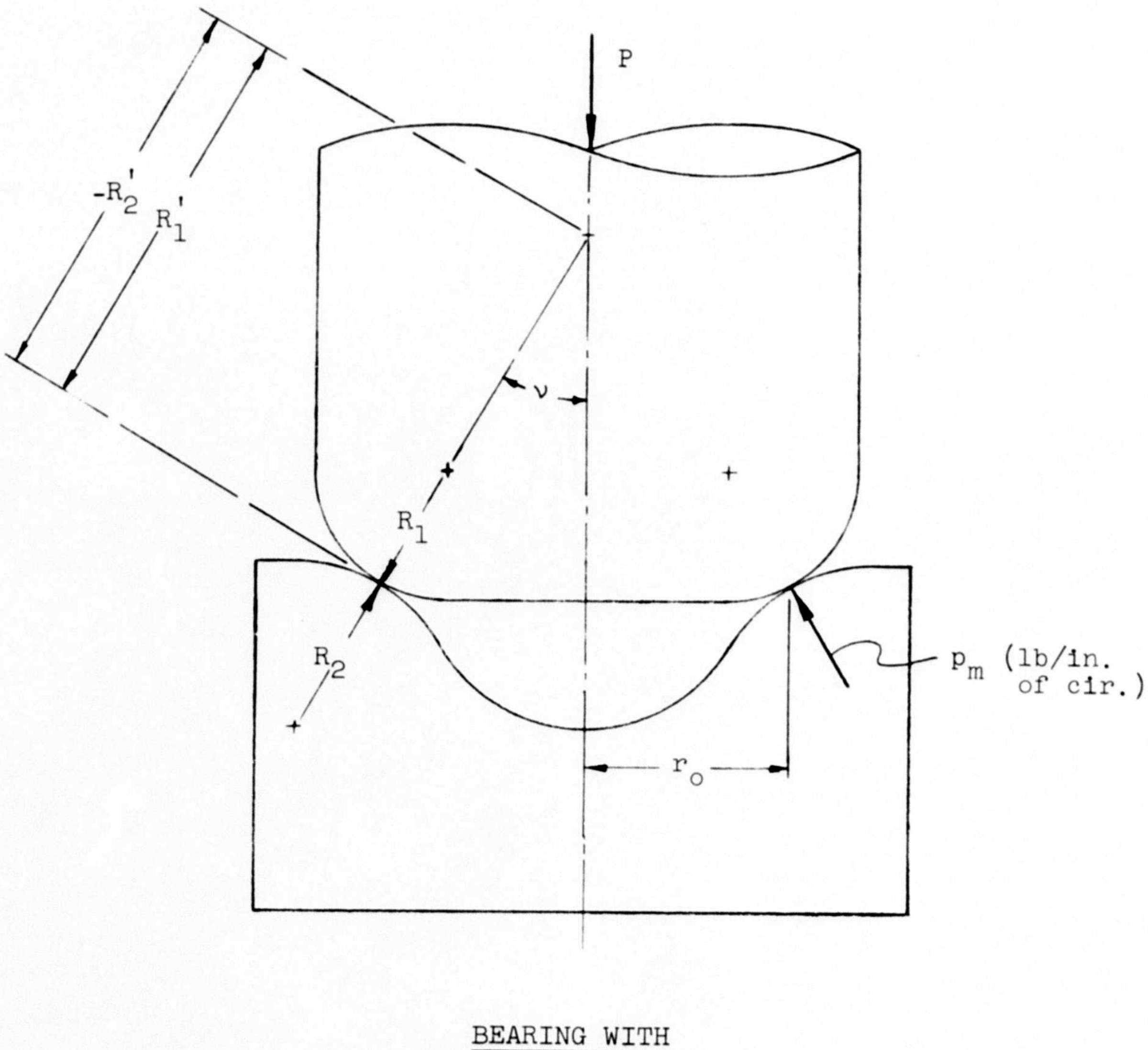

BEARING WITH

THEORETICAL LINE CONTACT

$$(120) \qquad B - A = \frac{1}{2}\left[\left(\frac{1}{R_1} - \frac{1}{R_1'}\right)^2 + 2\left(\frac{1}{R_1} - \frac{1}{R_1'}\right)\left(\frac{1}{R_2} - \frac{1}{-R_1'}\right)\cos[(2)(0)]\right.$$

$$\left. + \left(\frac{1}{R_2} - \frac{1}{-R_1'}\right)^2\right]^{1/2}$$

$$= \pm \frac{1}{2R_o}$$

and

$$(121) \qquad \cos\theta = \frac{B-A}{B+A} = \frac{\pm \frac{1}{2R_o}}{\frac{1}{2R_o}} = \pm 1$$

The minus sign has no significance and so θ is zero, and we verify that the surfaces conform in one direction.

Axial equilibrium gives the (uniformly distributed) normal force per unit length of contact as

$$(p_m)(2\pi r_o)(\cos\nu) = P$$

or

$$(28) \qquad p_m = \frac{P}{2\pi r_o \cos\nu} \text{ (lb/in of cir.)}$$

The maximum bearing pressure per unit area is given by

$$(124) \qquad q_o = \frac{2p_m}{\pi a}$$

where a is the small half width of the contact area and is given by

$$(125) \qquad a = \left[\frac{4\, p_m\, R_o}{\pi\, E_o}\right]^{1/2}$$

with R_o from Eq. 126 or 130, and E_o from Equation 131.

Eliminating p_m, a, and r_o from Eqs. 4, 28, 125, and 126 gives for the dimensionless relative bearing size D

$$(29) \qquad D = \frac{P^{1/2}\, E_o}{2(\pi)^{3/2}(q_o)^{3/2}\, R_o \cos\nu} = \left[\frac{P}{\pi q_o}\right]^{1/2} \left[\frac{E_o}{2\pi\, q_o\, R_o \cos\nu}\right]$$

For $\quad P = 15.95$ lb. (P. 114)

q_o = 285,000 psi (P. 108 - This choice is for theoretical line contact)

E_o = 21 x 10^6 psi (P. 108 - Sapphire jewel and steel shaft)

we have

$$D = \frac{P^{1/2} E_o}{2(\pi)^{3/2}(q_o)^{3/2}\, R_o \cos\nu}$$

(29)

$$= \frac{(15.95)^{1/2}(21 \times 10^6)}{(2)(3.14)^{3/2}(.285 \times 10^6)^{3/2}\, R_o \cos\nu}$$

$$= \frac{.0497}{R_o \cos\nu}$$

We see then that R_o should be as large as possible for small D (relative bearing size) and so should $\cos\nu$. This means that from the point of view of minimum bearing size as determined by axial load we want conforming surfaces (large R_o) normal to the axial load (large $\cos\nu$). For a typical bearing consider the spherical-conical bearing shown in Fig. 3. There

$$R_o = R$$

(30) $$\alpha = \nu$$

and $$R = r_o/\sin\alpha$$

Combining Eqs. 4, 5, 29, and 30 gives for this bearing

(31) $$D = \left[\frac{E_o \tan\alpha}{2\pi q_o}\right]^{1/2}$$

From this we see that the angle α should not be greater than say 45^o for this type of bearing. This is not only reasonable from a sizing point of view, but it also helps to prevent excessive circumferential stresses in the conical member due to the wedging action of the sphere in the cone.

For typical numerical sizes we have with

$E_o = 21 \times 10^6$ psi (P. 108)

q_o = 285,000 psi (P. 108)

α = 45° (Probable design maximum)

(31) $$D = \left[\frac{E_o \tan\alpha}{2\pi q_o}\right]^{1/2} = \left[\frac{(21 \times 10^6)\tan 45^\circ}{(2)(3.14)(.285 \times 10^6)}\right]^{1/2} = 3.42$$

$(d_o)_{ref}$ is calculated on the basis of a line contact design bearing stress of q_o = 285,000 psi.

Thus

$$(d_o)_{ref} = 2\left[\frac{P}{\pi q_o}\right]^{1/2} = 2\left[\frac{15.95}{(3.14)\quad(285,000)}\right]^{1/2} = .00843 \text{ in.}$$

and

$$d_o = D(d_o)_{ref} = (3.42)\quad(.00843) = .0288 \text{ in.}$$

This is not out of line with the values of d_o for conforming bearings (See Pages 15 and 16).

As a check and to determine if the eliminated quantities have reasonable magnitudes, we calculate these quantities for this example.

$$r_o = \frac{d_o}{2} = \frac{.0288}{2} = .0144$$

(28) $$p_m = \frac{P}{2\pi\, r_o \cos\nu} = \frac{15.95}{(2)\ (3.14)\ (.0144)\ \cos 45^\circ} = 250 \text{ lb./in.}$$

(30) $$R_o = \frac{r_o}{\sin\alpha} = \frac{(.0144)}{(.707)} = .0203 \text{ in.}$$

(31) $$D = \frac{.0497}{R_o \cos v} = \frac{.0497}{(.0203)(.707)} = \frac{.0497}{.0144} = 3.46$$

(124) $$a = \frac{2\, p_m}{\pi q_o} = \frac{(2)(250)}{(3.14)(285,000)} = .000559 \text{ in.}$$

(125) $$a = \left[\frac{4\, p_m\, R_o}{\pi\, E_o}\right]^{1/2} = \left[\frac{(4)(250)(.0203)}{(3.14)(21 \times 10^6)}\right]^{1/2} = .000554 \text{ in.}$$

As a comparison the cylinder enclosing the outermost limit of contact has a diameter of $d_o + 2a \cos\alpha$ = .0296 in. for this case. The sharp vee jewel bearing has for this cylinder's diameter (P. 119).

$$(2a')_{typ} = 2(.00516) = .01032 \text{ in.}$$

Thus for the same loads and materials, but with the potential ability to withstand transverse loads, we are about $\frac{.0296}{.01032} = 2.86$ times as large. This is quite reasonable. (Note that this is 2.86 times as large as the enlarged vee jewel. It still exceeds commercial practice on jewels, but the ratio is representative.)

BEARINGS WITH AXIAL LOAD CAPACITY - FRICTION TORQUE WHEN OPERATED UNDER AXIAL LOAD ALONE

Case 1 (See P. 7) The general expression for the friction torque on an annular area of radius r and meridian length ds, with coefficient of friction μ, and normal pressure q is

$$(32) \qquad dT_{fr} = \mu q(2\pi r)(ds)(r)$$

For Case 1: $q(r) = q_o$, $ds = dr$, and the limits of integration are $r = r_1$ and $r = r_o$. Thus

$$T_{fr} = \int_{r=r_1}^{r=r_o} dT_{fr}(r) = \int_{r_1}^{r_o} 2\pi\mu q_o \, r^2 dr$$

$$= \frac{2\pi\mu \, q_o}{3} [r_o^3 - r_1^3]$$

We define as a reference friction torque the torque on a solid flat bearing with uniform normal pressure distribution. Since $r_1 = 0$ and $r_o = (r_o)_{ref}$ (Eq. 4), we have for this case

$$(34) \qquad (T_{fr})_{ref} = \frac{2\pi\mu \, q_o}{3} [(r_o)_{ref}]^3 = \frac{2}{3} (\mu P) \, (r_o)_{ref}$$

It then seems natural to define a reference friction radius as

$$(35) \qquad (r_{fr})_{ref} = \frac{2}{3}(r_o)_{ref} = \frac{2}{3}\left[\frac{P}{\pi q_o}\right]^{1/2} = \frac{(T_{fr})_{ref}}{\mu P}$$

and a bearing friction radius ratio Δ by

$$(36) \qquad \Delta = \frac{r_{fr}}{(r_{fr})_{ref}}$$

and

$$(37) \qquad r_{fr} = \frac{T_{fr}}{\mu P}$$

Using these definitions gives for Δ in terms of β (when Eq.7 for $D(\beta)$ is considered)

$$(38) \qquad \Delta(\beta) = \frac{\beta^3 - 1}{(\beta^2 - 1)^{3/2}}$$

As β approaches infinity this approaches 1, as it should for the solid flat bearing. This function is tabulated below in Table 5 and plotted in Figure 14.

Table 5

FRICTION RADIUS RATIO Λ VS BEARING RADIUS RATIO β FOR A UNIFORM LOAD ON A HOLLOW FLAT BEARING

β	$\Lambda(\beta)$
∞	1.000
10	1.019
5	1.058
3	1.150
2	1.348
5/3	1.530
5/4	2.26
10/9	3.28

From the plot we note that $\Lambda(\beta)$ increases more rapidly than $D(\beta)$ in the range of β of interest.

Case 2 (See Page 12) In Eq. 32 $q(r)$ is given by Eq. 8, $ds = dr$, and the limits of integration are r_i and r_o. Thus we get for the friction torque

$$T_{fr} = \int_{r_i}^{r_o} dT_{fr}(r) = \int_{r_i}^{r_o} (2\pi\mu)(q_o)\left(1 - \frac{r - r_i}{r_o - r_i}\right)r^2 dr$$

FIGURE XIV

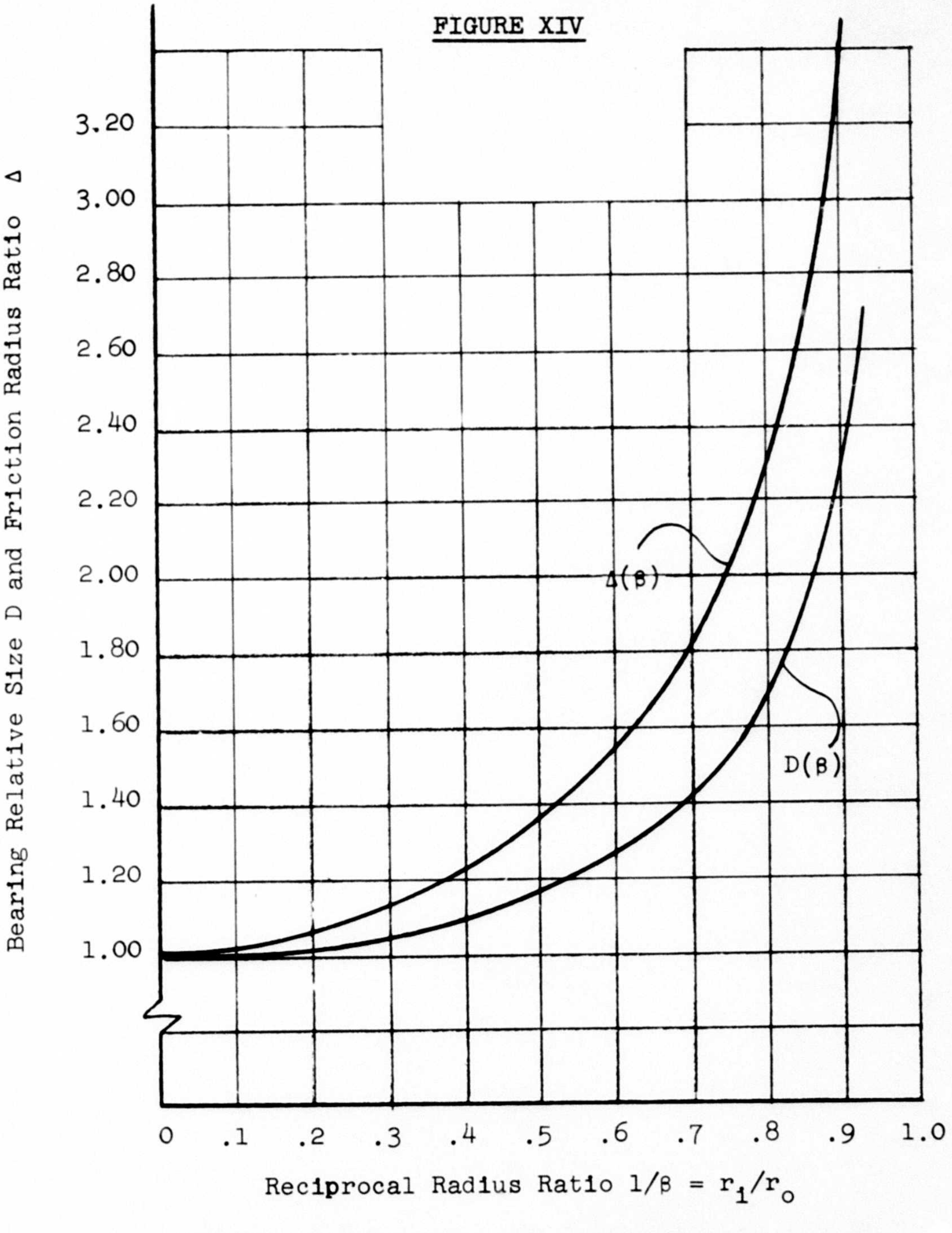

BEARING RELATIVE SIZE D AND FRICTION RADIUS RATIO VS. RECIPROCAL RADIUS RATIO 1/β FOR A HOLLOW FLAT BEARING WITH A UNIFORM PRESSURE DISTRIBUTION

(39)

$$= 2\pi\mu q_o \left[\frac{r_o^3 - r_1^3}{3} - \frac{1}{r_o - r_1} \left(\frac{r_o^4}{4} - \frac{r_1 r_o^3}{3} + \frac{r_1^4}{12} \right) \right]$$

The dimensionless friction radius ratio Λ becomes

(40) $$\Delta(\beta, \eta) = \Delta(D(\beta, \eta), \beta) = D^3 \left[1 - \frac{1}{\beta^3} - \eta \, \frac{3\beta/4 - 1 + 1/4\beta^3}{\beta - 1} \right]$$

where $D(\beta, \eta)$ is given by Equation 10. Rather than plot this we evaluate it for a typical case. Taking $\eta = .5$ (trapezoidal distribution) and $\beta = 1.667$ we have (See P. 14)

$$D(1.667, .5) = 1.463$$

and

$$\Delta(1.667, .5) = (1.463)^3 (.556) = 1.74$$

We compare this to $\Delta(1.667, 0) = 1.530$ (P. 39) and see that for the trapezoidal distribution the friction radius increases by a factor of $1.74/1.53 = 1.14$ over that for a uniform distribution with the same axial load, design bearing stress, and radius ratio.

<u>Case 3</u> (See P. 16) In Eq. 32, $q(\theta) = q_o$, $ds = Rd\theta$, and the limits of integration are $\theta = 0$ and $\theta = \alpha$. Thus we get for the friction torque

$$T_{fr} = \int_{\theta=0}^{\theta=\alpha} dT_{fr}(\theta) = \int_0^{\alpha} \mu\, q_o\, [2\pi r(\theta)](R\,d\theta)[r(\theta)]$$

where $r(\theta)$ and R are related to θ and α by Eqs. 11 and 12. Integrating gives

$$(41) \qquad T_{fr} = 2\pi\mu q_o \frac{r_o^3}{\sin^3\alpha}\left[\frac{\alpha}{2} - \frac{\sin 2\alpha}{4}\right]$$

and the dimensionless friction ratio becomes

$$(42) \qquad \Delta(\alpha, D(\alpha)) = D^3\left[\frac{3\alpha}{2\sin^3\alpha} - \frac{3\sin 2\alpha}{4\sin^3\alpha}\right]$$

where D = 1 for this case. For a typical size take $\alpha = 30^\circ$. Then $\Delta(30^\circ) = 1.08$. So for $\alpha = 30^\circ$ the friction radius for this case is 1.08 times as high as for a flat bearing.

Case 4 (See P. 18) Only the limits of integration change from Case 3. The lower limit becomes $\theta = \alpha_1$ giving

$$(43) \qquad T_{fr} = 2\pi\mu q_o \frac{r_o^3}{\sin^3\alpha}\left[\frac{\alpha}{2} - \frac{\sin 2\alpha}{4} - \frac{\alpha_1}{2} + \frac{\sin 2\alpha_1}{4}\right]$$

The dimensionless friction ratio becomes

$$(44) \qquad \Delta[\alpha, \alpha_1, D(\alpha, \alpha_1)] = D^3 \frac{3}{2\sin^3\alpha}\left[\alpha - \alpha_1 - \frac{\sin 2\alpha - \sin 2\alpha_1}{2}\right]$$

In Equation 44, D^3 is the same as for a flat bearing with uniform normal pressure (Eq. 7) and α_1, α, and β are related by Eq. 19. For a typical size take

$$\alpha = 90^\circ \text{ and } \beta = 1.667$$

Then

$$(19) \qquad \sin\alpha_1 = \frac{1}{\beta}\sin\alpha = (.6)(1) = .6, \quad \alpha_1 = 36.8^\circ$$

and

$$D^3 = (1.250)^3 \text{ (P. 14)}$$

and

$$\Delta = (1.953)(1.5)(1.408) = 4.12$$

This is high, but a uniform normal pressure distribution from $\alpha_1 = 36.8^\circ$ to $\alpha = 90^\circ$ gives a large friction effect from that part of the arc near $\theta = 90^\circ$ with little or no effect on the axial load. We should expect the cosine normal pressure distribution of Case 6 to give more realistic values here.

<u>Case 5</u> (P. 18) Here

$$q(\theta) = q_o \cos\theta$$
$$ds = R\, d\theta$$
$$r = R \sin\theta$$
$$r_o = R \sin\alpha$$

and Eq. 32 becomes

$$dT_{fr} = (\mu)(q_o \cos\theta)(2\pi R \sin\theta)(R\, d\theta)(R\sin\theta)$$

The limits are $\theta = 0$ and $\theta = \alpha$. Thus

$$T_{fr} = \int_0^{\alpha} dT_{fr}(\theta) = \int_0^{\alpha} \mu q_o\, 2\pi R^3 \sin^2\theta \cos\theta\, d\theta$$

or

(45) $$T_{fr} = \frac{2\pi\mu q_o\, r_o^3}{3}$$

The dimensionless friction radius ratio becomes

(46) $$\Delta = D^3$$

where $D(\alpha)$ is given by Eq. 15 and is tabulated on P. 20.

For numerical values take $\alpha = 90^o$. Then

$$D(\alpha) = \left[\frac{3}{2}\right]^{1/2} = 1.225 \quad \text{(P. 20)}$$

and

$$\Delta(90^o) = 1.838$$

Thus the solid hemispherical bearing with a cosine normal pressure distribution has only 1.225 times the outside diameter of a flat bearing of the same capacity, but has 1.838 times as much friction torque.

<u>Case 6</u> (P. 22) Here $q(\theta) = q_o \cos\theta/\cos\alpha_1$ and the lower limit becomes α_1 where $\sin \alpha_1 = r_1/R$ (Eq. 17). The friction torque becomes

$$T_{fr} = \int_{\alpha_1}^{\alpha} dT_{fr}(\theta) = \int_{\alpha_1}^{\alpha} \frac{\mu q_o \ 2\pi R^3}{\cos\alpha_1} \sin^2\theta \cos\theta \, d\theta$$

or

(47) $$T_{fr} = \frac{2\pi\mu q_o \ r_o^3}{3 \cos\alpha_1} \left[1 - \frac{1}{\beta^3}\right]$$

The friction radius ratio then becomes

(48) $$\Delta(\beta, D, \alpha_1) = \frac{D^3 \left(1 - \frac{1}{\beta^3}\right)}{\cos \alpha_1}$$

For typical numerical values take $\alpha = 90^o$ and $\beta = 1.667$. Then (P. 25) $\alpha_1 = 36.8^o$ and $D = 1.532$ giving

$$\Delta = \frac{D^3 \left(1 - \frac{1}{\beta^3}\right)}{\cos\alpha_1} = \frac{(1.532)^3(1 - .6^3)}{.8} = 3.52$$

Thus the size is 1.532 times that of a solid flat bearing, but the friction torque is 3.52 times as much.

Case 7 (P. 25) Here

(20) $q(\theta) = q_o$

(21) $r(\theta) = r_1 + R \sin\theta$

and
(22) $R = \dfrac{r_o - r_1}{\sin\alpha}$

The limits of integration are $\theta = 0$ and $\theta = \alpha$, and $ds = R\, d\theta$. The friction torque thus becomes

$$T_{fr} = \int_{\theta=0}^{\theta=\alpha} dT_{fr}(\theta) = \int_0^{\alpha} (\mu)(q_o)(2\pi)(r_1 + R \sin\theta)^2 R\, d\theta$$

which upon integration gives

(49) $$T_{fr} = 2\pi\mu q_o R \left[r_1^{\,2} + 2\, r_1 R(1 - \cos\alpha) + R^2\left(\frac{\alpha}{2} - \frac{\sin 2\alpha}{4}\right) \right]$$

The friction radius ratio then becomes

(50) $$\Delta = D^3 \frac{3(1 - \frac{1}{\beta})}{\sin\alpha} \left[\frac{\alpha}{\beta^2} + \frac{2(1 - \cos\alpha)}{\sin\alpha} \frac{1}{\beta}(1 - \frac{1}{\beta}) + \frac{(\frac{\alpha}{2} - \frac{\sin 2\alpha}{4})}{\sin^2\alpha}(1 - \frac{1}{\beta})^2\right]$$

For numerical values in a particular case take $\alpha = 90°$ and $\beta = 1.667$. Then

$$D = 1.250 \text{ (P. 14)}$$

and

$$\Delta = (1.250)^3 \left[(3)(\frac{.4}{1}) \left[\frac{\pi(9)}{2(25)} + \frac{2(1 - 0)}{1} (.6)(.4) + \frac{\frac{\pi}{4} - \frac{0}{4}}{(1)^2} (.4)^2\right]\right]$$

$$\Delta = 1.250^3 \ (1.42) = 2.77$$

We see that the combination of a uniform pressure distribution and $\alpha = 90°$ gives large weight to friction on the outer arc length that is nearly parallel to the centerline (AB in the sketch, Fig. 15) and so tends to make the friction torque high.

<u>Case 8</u> (P. 27) This is the same as Case 7 except that

(25) $$q(\theta) = q_o \cos\theta$$

The friction torque is then

FIGURE XV

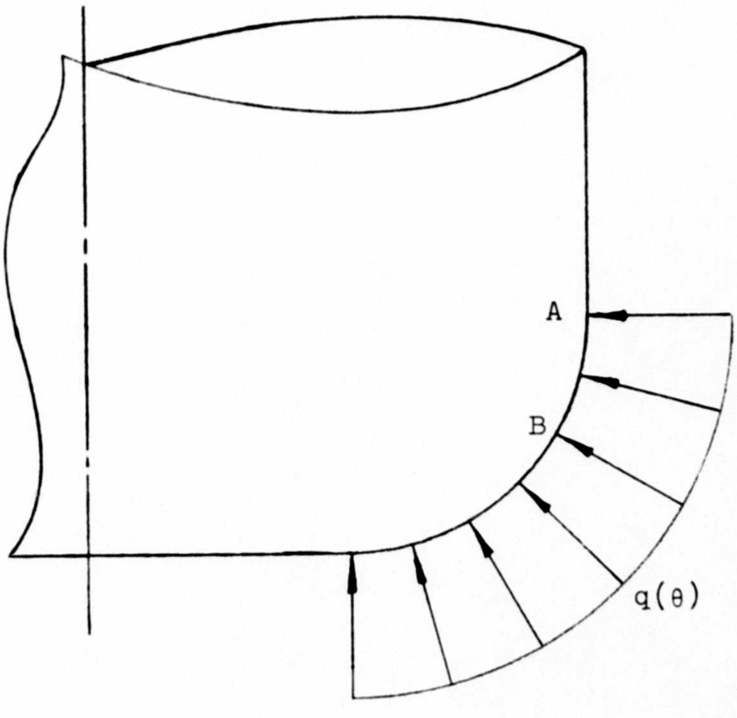

EFFECT OF LARGE NORMAL

PRESSURES NEAR $\alpha = 90^{\circ}$

$$T_{fr} = \int_0^\alpha dT_{fr}(\theta) = \int_0^\alpha (\mu)(q_o \cos\theta)(2\pi)(r_1 + R\sin\theta)^2 R\, d\theta$$

which upon integration gives

(51) $$T_{fr} = 2\pi\mu\, q_o R \left[r_1^2 \sin\alpha + r_1 R \sin^2\alpha + R^2 \frac{\sin^3\alpha}{3} \right]$$

The friction radius ratio then becomes

(52) $$\Delta = D^3 \left[1 - \frac{1}{\beta^3} \right]$$

Note that even though Eq. 38 can be put into this form, $D(\beta)$ in Eq. 38 is given by Eq. 7 while $D(\beta)$ here is given by Eq. 27 and is larger.

For the numerical values in a particular case take $\alpha = 90^\circ$ and $\beta = 1.667$. Then $D(\beta,\alpha) = 1.695$ (P. 28) and $\Delta(\beta) = (1.695)^3 [1 - .6^3] = 3.81$. Comparing Cases 4, 6, 7, and 8 with $\beta = 5/3$ and $\alpha = 90^\circ$ gives

	$D(\beta = 5/3, \alpha = 90^\circ)$	$\Delta(5/3, 90^\circ)$
Case 4 - Hollow sph. unif. pres.	1.250	4.12 (P. 43)
Case 6 - Hollow sph. cosine pres.	1.532	3.52 (. 46)
Case 7 - Hollow torr. unif. pres.	1.250	2.77 (P. 47)
Case 8 - Hollow torr. cosine pres.	1.695	3.81 (P. 49)

The uniform pressure assumption is seen to be more conservative as regards friction torque for the spherical bearing, but not for the torroidal bearing; and the cosine pressure assumption is more conservative as regards size for both cases. The cosine pressure assumption is more realistic for both shapes and with this we see that for the angle $\alpha = 90^{\circ}$ and $\rho = 1.667$ the hollow spherical bearing has both smaller size and lower friction than the hollow torroidal bearing.

Case 9 (P. 28) Here

$$q(r) = q_o$$

$$ds = dr/\cos\nu$$

and the limits of integration are r_1 and r_o. The friction torque becomes

$$T_{fr} = \int_{r_1}^{r_o} dT_{fr}(r) = \int_{r_1}^{r_o} \mu(q_o)(2\pi r)(\frac{dr}{\cos\nu})(r)$$

which upon integration gives

$$(53) \qquad T_{fr} = \frac{2\pi\mu q_o}{\cos\nu} \frac{(r_o^3 - r_1^3)}{3}$$

The friction radius ratio becomes

(54) $$\Lambda = D^3 \left(1 - \frac{1}{\beta^3}\right) \frac{1}{\cos\nu}$$

Thus while the size of this conical bearing is the same as for a flat bearing, the friction torque increases by a factor of $\frac{1}{\cos\nu}$.

The largest ν used would probably not exceed 45° due to the wedging that would occur. Thus for $\nu = 45^\circ$ and $\beta = 1.667$, $\Lambda = 1.414$ times that of the flat bearing with the same β or (See P. 39 for 1.530).

$$\Lambda\left(\beta = \frac{5}{3},\ \nu = 45^\circ\right) = (1.414)\ (1.530) = 2.17$$

Case 10 (See P. 30) In this case the normal forces are all acting at the radius r_o so that

$$T_{fr} = (\mu)(p_m)(2\pi r_o)(r_o)$$

Using Eq. 28 for p_m gives

(55) $$T_{fr} = \mu P\ r_o/\cos\nu$$

The friction radius ratio then becomes

(56) $$\Lambda = \frac{3}{2}\frac{D}{\cos\nu}$$

For the spherical-conical bearing shown in Fig. 3, (P. 6) with the numerical values of Pages 34 and 35, we have (See P. 35 for D)

$$\Lambda = \frac{3}{2} \frac{(2.42)}{\cos 45^{\circ}} = 7.24$$

While this seems high note on P. 36 that this bearing is about 2.86 times as large as a flat bearing with the same materials and axial load capacity.

In all of the cases above we are probably not too worried about high friction torques due to axial loads as these loads are only acting a relatively short time and the mechanism may not even be required to operate during the axial acceleration interval. The results above are included mainly for completeness.

SECTION II

TRANSVERSE LOADING ON BEARINGS WITH AXIAL LOAD CAPACITY

General Procedure

A reasonable distribution of normal forces will be assumed for each of the bearing shapes, and the friction torque and transverse force will each be found in terms of the maximum normal contact pressure. This will allow the friction torque and maximum contact pressure to be expressed in terms of the transverse applied force.

Cases 1 and 2 - Flat Bearings

These flat bearings cannot resist transverse load. They were analyzed because they provide the most resistance to axial load and so form a standard for the other bearings, and because they can be used in conjunction with journal bearings which are studied in SECTION III.

Cases 3, 4, 5, and 6 - Spherical Bearings - Hollow and Solid

Only one normal pressure distribution will be considered for spherical bearings under transverse load. Solid bearings will be considered as a special case of hollow ones. Figure 16 shows the bearing and the parameters of interest.

The normal pressure has been taken to be a function of the latitude angle θ and the longitude angle ϕ. As a reasonable distribution for initially conforming surfaces such as these we assume

FIGURE XVI

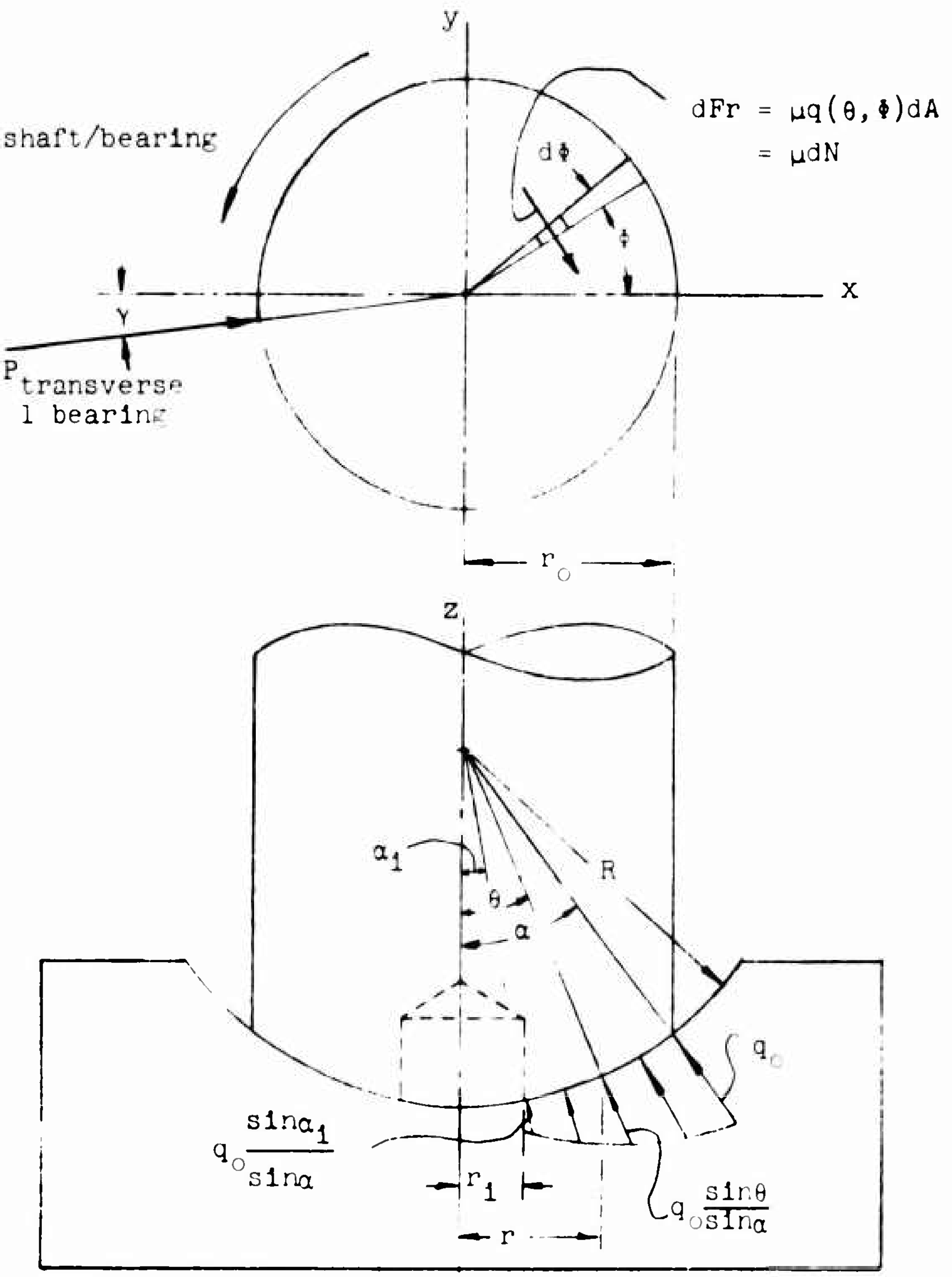

SPHERICAL BEARING FOR

TRANSVERSE LOAD ANALYSIS

$$(57) \qquad q(\theta,\phi) = q_o \frac{\sin\theta}{\sin\alpha}\cos\phi \qquad \begin{array}{c} \alpha_1 \le \theta \le \alpha \\ -\frac{\pi}{2} \le \phi \le \frac{\pi}{2} \end{array}$$

This distribution is sketched in Fig. 16 as a function of θ for $\phi = 0$. For any other ϕ between $-\frac{\pi}{2}$ and $\frac{\pi}{2}$ the variation with θ is the same, but all values are scaled down by the factor $\cos\phi$. The longitude of maximum normal pressure is taken behind the plane of the transverse applied load by an acute angle γ as shown. At a fixed latitude θ, the pressure is assumed to drop off harmonically with longitude ϕ from this maximum value. Similarly at a fixed longitude ϕ the pressure is assumed to vary harmonically with θ, being maximum when θ is maximum. The angle γ is caused by the transverse resultant friction force as will be seen below.

The angles and radii are related by:

(11) $\quad r = R\sin\theta$

(12) $\quad r_o = R\sin\alpha$

(17) $\quad r_1 = R\sin\alpha_1$

and the radius ratio β is

$$(19) \qquad \beta(\alpha) = \frac{\sin\alpha}{\sin\alpha_1} = \frac{r_o}{r_1}$$

The differential element of area is

(58) $$dA = (R d\theta)(r d\phi)$$

The friction torque due to the normal pressure $q(\theta)$ on the area dA is

(59) $$dT_{fr} = \mu q(\theta,\phi)(dA)(r(\theta)) = (\mu)(dN)(r)$$

which, when equations 11, 12, 17, 57, and 58 are used can be written as

$$dT_{fr}(\theta,\phi) = \frac{\mu q_o \sin\theta \cos\phi (R d\theta)(R\sin\theta d\phi)(R\sin\theta)}{\sin\alpha}$$

or

(60) $$dT_{fr}(\theta,\phi) = \frac{\mu q_o r_o^3}{\sin^4\alpha} (\sin^3\theta \cos\phi)\, d\theta d\phi$$

Then the friction torque becomes

$$T_{fr} = \int_{\theta=\alpha_1}^{\theta=\alpha} \int_{\phi=-\frac{\pi}{2}}^{\phi=\frac{\pi}{2}} dT_{fr}(\theta,\phi)$$

or

(61) $$T_{fr}(q_o,\alpha,\alpha_1) =$$

$$\frac{2\mu q_o r_o^3 \left[\cos\alpha_1 \sin^2\alpha_1 - \cos\alpha \sin^2\alpha + 2(\cos\alpha_1 - \cos\alpha)\right]}{3\sin^4\alpha}$$

In order to find q_o in terms of the transverse load applied to the bearing we must find the transverse components of dN and dFr and write the transverse equations of equilibrium.

From the symmetry of $q(\theta, \phi)$ about the xz plane we see that the distribution $q(\theta, \phi)$ has zero Y_n component. Its X_n component is given by

$$(62) \qquad -X_n = \int_{\theta=\alpha_1}^{\theta=\alpha} \int_{\phi=-\frac{\pi}{2}}^{\phi=\frac{\pi}{2}} (q(\theta, \phi)dA)(\sin\theta)(\cos\phi)$$

which upon integration becomes

$$(63) \qquad -X_n = \frac{\pi q_o r_o^2}{6 \sin^3\alpha} \left[(\cos\alpha_1 \sin^2\alpha_1 - \cos\alpha \sin^2\alpha) + 2(\cos\alpha_1 - \cos\alpha) \right]$$

The symmetry of $q(\theta, \phi)$ about the xz plane also gives zero X_{fr} component of the friction force. Its Y_{fr} component is given by

$$(64) \qquad -Y_{fr} = \int_{\theta=\alpha_1}^{\theta=\alpha} \int_{\phi=-\frac{\pi}{2}}^{\phi=\frac{\pi}{2}} \mu q(\theta, \phi)dA \cos\phi$$

which upon integration becomes

$$(65)\qquad -Y_{fr} = \frac{\pi\mu q_o r_o^2}{4\sin^3\alpha}\left[(\alpha - \alpha_1) - \frac{1}{2}(\sin 2\alpha - \sin 2\alpha_1)\right]$$

The equilibrium of forces parallel to the xy plane then gives

$$(66)\qquad P_{tr.1\ brg.} = \left[(-X_n)^2 + (-Y_{fr})^2\right]^{1/2}$$

and

$$(67)\qquad \tan\gamma = \frac{-Y_{fr}}{-X_n}$$

which can be used to express γ in terms of the geometric quantities α and α_1 and the coeficient of friction μ. Of more interest, however, is the relation between $P_{tr.1\ brg.}$ and q_o, which can be written as

$$(68)\qquad P_{tr.1\ brg.} = \left[\frac{\pi\, q_o r_o^2}{\sin^3\alpha}\right]\left[(A^2(\alpha,\alpha_1) + \mu^2 B^2(\alpha,\alpha_1)\right]^{1/2}$$

where

$$(69)\qquad A(\alpha,\alpha_1) = \frac{1}{6}\left[(\cos\alpha_1 \sin^2\alpha_1 - \cos\alpha \sin^2\alpha) + 2(\cos\alpha_1 - \cos\alpha)\right]$$

$$(70)\qquad B(\alpha,\alpha_1) = \frac{1}{4}\left[(\alpha - \alpha_1) - \frac{1}{2}(\sin 2\alpha - \sin 2\alpha_1)\right]$$

and

(70a) $\tan\gamma = \frac{\mu B}{A}$

To make the results dimensionless we introduce a reference transverse outside radius $(r_o)_{ref.\ tr.}$, such that the transverse load on one bearing divided by the area of a semicircle of this radius gives q_o. Thus

(71) $$(r_o)_{ref.tr.} = \left[\frac{2P_{tr.\ 1\ brg.}}{\pi\ q_o}\right]^{1/2} = \left[\frac{P_{tr.\ shaft}}{\pi\ q_o}\right]^{1/2}$$

(Note the similarity in form to Eq. 4, P. 7.) Then we define the transverse size ratio as

(72) $$D_{tr} = \frac{r_o}{(r_o)_{ref.tr.}}$$

(Note that $D_{tr} = 1$ for $\alpha = 90^o$, $\alpha_1 = 0^o$, and $q(\theta,\phi) = q_o$; and compare to Case 3 where D = 1.)

Using these definitions Equation 68 becomes

(73) $$D_{tr} = \left[\frac{\sin^3\gamma}{2(A^2 + \mu^2B^2)^{1/2}}\right]^{1/2}$$

Next a transverse friction radius is introduced by

$$(74) \qquad r_{fr.\ tr.} = \frac{T_{fr.1\ brg.}}{\mu\ P_{tr.1\ brg.}}$$

and a reference transverse friction radius by

$$(75) \qquad r_{fr.\ ref.tr.} = \frac{\pi}{2}\ (r_o)\ ref.\ tr.$$

A cylinder of radius r_o and length h with uniform pressure q_o over half of its circumference has a friction torque of $T_{fr} = \mu q_o \pi r_o h r_o$ and a transverse load of $P_{tr.1\ brg.} = q_o(2r_o h)$. Its transverse friction radius is then $r_{fr.tr.cyl.} = T_{fr}/(\mu P_{tr.})$ $= \pi r_o/2$. Both $(r_o)_{ref.\ tr.}$ and $r_{fr.\ ref.\ tr.}$ are quite artificia

Finally, a transverse friction radius ratio $\Delta_{tr.}$ is introduced as

$$(76) \qquad \Delta_{tr.} = \frac{r_{fr.tr.}}{r_{fr.ref.tr.}} = \frac{r_{fr.tr.}}{\frac{\pi}{2}\ r_{o\ ref.\ tr.}} = \frac{2}{\pi} \frac{T_{fr.1\ brg.}}{\mu\ P_{tr.\ 1brg.}\ r_{o\ ref.}}$$

Combining these definitions with the expressions for $T_{fr.}$ and $P_{tr.}$ in terms of q_o gives

$$(77) \qquad \Delta_{tr.} = \frac{8}{\pi^2\ \sin\alpha} \left[\frac{A}{A^2 + \mu^2 B^2}\right]^{1/2} \left[D_{tr.}\right]$$

or

(78) $$\Lambda_{tr} = \frac{8\cos\gamma}{\pi^2 \sin\alpha}(\Omega_{tr})$$

when Eq. 67 is used.

For numerical values consider the 4 cases:

$$\alpha = 90^\circ \quad \text{with} \quad \beta = \infty \quad \text{and} \quad \beta = 5/3$$

and

$$\alpha = 30^\circ \quad \text{with} \quad \beta = \infty \quad \text{and} \quad \beta = 5/3$$

where $\mu = .17$ (P. 122).

<u>($\alpha = 90^\circ$, $\beta = \infty$)</u> (Full solid hemispherical bearing)

$$\alpha_1 = 0^\circ$$

(69) $$A(\alpha,\alpha_1) = \frac{1}{6}[(0 - 0) + 2(1 - 0)]$$

$$= .333$$

(70) $$\mu B(\alpha,\alpha_1) = \frac{.17}{4}[(\frac{\pi}{2} - 0) - \frac{1}{2}(\sin\pi - \sin 0)]$$

$$= \frac{.17\pi}{8} = .0667$$

$$\tan\gamma = \frac{\mu B}{A} = .200$$

(70a) $\gamma = 11.33^{\circ} = .198$ rad.

$\cos\gamma = .980$

(73) $$D_{tr} = \frac{[\sin^3\gamma]^{1/2}}{[2]^{1/2}[A^2 + (\mu B)^2]^{1/4}} = \frac{1}{1.414}\left[\frac{\cos\alpha}{A}\right]^{1/2}$$

$$= \frac{1}{1.414}\left(\frac{.980}{.333}\right)^{1/2}$$

$D_{tr} = 1.212$

<u>$\alpha = 90^{\circ}$, $\beta = 1.667$</u> (Hollow hemispherical bearing)

$\alpha_1 = 36.8^{\circ}$ (P. 25)

$$A(\alpha,\alpha_1) = \frac{1}{6}\left[((.8)(.6)^2 - 0) + 2(.8 - 0)\right] = .314$$

$$\mu B(\alpha,\alpha_1) = \frac{.17}{4}\left[(\frac{\pi}{2} - .642) - \frac{1}{2}(0 - \sin 73.6^{\circ})\right] = .0599$$

$$\tan\gamma = \frac{.0599}{.314} = .291$$

$\gamma = 10.8^{\circ} = .188$ rad.

$\cos\gamma = .984$

$$D_{tr} = \frac{1}{1.414}\left(\frac{.984}{.313}\right)^{1/2} = 1.250$$

This small increase indicates that the section from $\theta = 0$ to $\theta = \alpha_1 = 36.8^{\circ}$ does not carry much transverse load when $\alpha = 90^{\circ}$. This seems reasonable.

$\alpha = 30^o,\ \beta = \infty$ (Solid bearing with outside half angle of 30^o)

$$\alpha_1 = 0$$

$$A(\alpha,\alpha_1) = \frac{1}{6}\,[(0 - (.866)(.5)^2) + 2(1 - .866)] = .00859$$

$$uB = \frac{.17}{4}\,[(\frac{\pi}{6} - 0) - (.5(\sin 60^o - \sin 0^o)] = .00387$$

$$\tan\gamma = \frac{.00387}{.00859} = .451$$

$$\gamma = 24.23^o$$

$$\cos\gamma = .911$$

$$D_{tr} = \left[\frac{\cos\gamma}{2A}\sin^3\alpha\right]^{1/2} = \left[\frac{.911}{.00859}\right]^{1/2}\frac{1}{1.414}\,(.5)^{3/2} = 2.58$$

(This relatively high value of D_{tr} may control sizing. Check below.)

$\alpha = 30^o,\ \beta = 1.667$ (Hollow bearing with outside half angle of 30^o)

$$\alpha_1 = 17.47^o = .305 \text{ rad.} \quad \text{(P. 24)}$$

$$A = \frac{1}{6}\,[(\cos 17.47^o \sin^2 17.47^o - .2165$$

$$+ 2(\cos 17.47^o - .866)] = .00790$$

$$uB = \frac{.17}{4}\,[(\frac{\pi}{6} - .305) - .5\,(.866 - \sin 34.94^o)] = .00308$$

$$\tan\gamma = \frac{.00308}{.00790} = .390$$

$\gamma = 21.3^{\circ}$

$\cos\gamma = .931$

$$D_{tr.} = \left[\frac{.931}{.00790}\right]^{1/2} \frac{(.5)^{3/2}}{(1.414)} = 2.71$$

The relatively high values of $D_{tr.}$ for $\alpha = 30^{\circ}$ may control sizing. To check this we go to the definitions of $D_{tr.}$ and D to get

(78) $$(D_{tr})_{\substack{\text{Maximum allow-}\\ \text{able for axial}\\ \text{loading to con-}\\ \text{trol sizing}}} = D_{design} \left[\frac{P_{axial\ design}}{(P_{tr})_{Total\ design}} \frac{(q_o)_{tr.\ design}}{(q_o)_{axial\ design}}\right]^{1/2}$$

Using the numerical values:

$P_{axial\ design}$ = 15.95 lb. (P. 114)

$P_{tr\ total\ design}$ = 8.87 lb. (P 124)

$q_{o\ axial\ design}$ = 242,000 pxi (P. 95)

$(q_o)_{tr.\ design}$ = 242,000 psi (P. 95) noting that

the bearing must allow rotation under the transverse load),

gives for the four cases considered:

$\alpha = 90^\circ, \beta = \infty$

$\alpha_1 = 0; \quad D(\alpha, \alpha_1) = 1.225$ (cosine load P. 25)

$$D_{\substack{tr.\ max. \\ allow.}} = 1.225 \left[\frac{15.95}{8.87} \times \frac{242{,}000}{242{,}000} \right]^{1/2} = (1.225)(1.80)^{1/2}$$

(77)

$$D_{\substack{tr.\ max. \\ allow.}} = 1.225(1.342) = 1.642$$

Thus the sizing is controlled by the axial-loading for this bearing and loading. ($D_{tr.} = 1.212$ (P. 62))

$\alpha = 90^\circ, \beta = 1.667$

$\alpha_1 = 36.8^\circ$, $D = 1.532$ (cosine load P. 25)

$$D_{\substack{tr.\ max. \\ allow.}} = 1.532\ (1.342) = 2.06$$

Here the sizing is still controlled by the axial load. ($D_{tr.} = 1.250$, P. 62)

$\alpha = 30^\circ, \beta = \infty$

$\alpha_1 = 0$, $D = 1.036$ (cosine load, P. 24)

$$D_{\substack{tr.\ max. \\ allow.}} = (1.035)\ (1.342) = 1.390$$

$\underline{\alpha = 30^\circ \ \beta = 1.667}$

$$\alpha_1 = 17.47^\circ, \ D = 1.283 \quad (P. 24)$$

$$\nu_{tr.\ max.\ allow.} = (1.283)(1.342) = 1.723$$

In these last two cases the transverse loading definitely controls sizing ($D_{tr.} = 2.58$ and $D_{tr.} = 2.71$ respectively, Pages 63, 64).

The main general conclusion about the relative suitability of shallow ($\alpha = 30^\circ$) spherical bearings is then that the design axial load must be much higher than the design transverse loads. In any particular design of course, the actual load ratios may depart from those that were used here.

For the numerical calculation of $\Delta_{tr.}$ we have (Eq. 78):

$\underline{\alpha = 90^\circ, \ \beta = \infty}$ $\cos\gamma = .980$ (P. 62)

$$\Delta_{tr.} = \frac{8\ (.980)\ (1.212)}{\pi^2 \quad (1)} = (.795)(1.212) = .964$$

$\underline{\alpha = 90^\circ, \ \beta = 1.667}$ $\cos\gamma = .984$ (P. 62)

$$\Delta_{tr.} = \frac{8\ (.984)\ (1.250)}{\pi^2 \quad (1)} = (.798)(1.250) = .998$$

$\underline{\alpha = 30^\circ, \ \beta = \infty}$ $\cos\gamma = .911$ (P. 63)

$$\Lambda_{tr.} = \frac{8}{\pi^2} \frac{(.911)(2.58)}{(.5)} = (1.48)(2.58) = 3.82$$

$\alpha = 30^\circ,\ \beta = 1.667$ $\cos\gamma = .931$ (P. 64)

$$\Lambda_{tr} = \frac{8}{\pi^2} \frac{(.931)(2.71)}{(.5)} = (1.51)(2.71) = 4.09$$

These results indicate less friction torque when $\alpha = 90^\circ$ than when $\alpha = 30^\circ$, and also only a very small increase in friction torque for hollow spherical bearings over solid ones with the same outside angle.

It would be of interest to have a numerical value for the operating friction torque. Let us consider the case:

$\alpha = 90^\circ,\ \beta = \infty$

We have $D_{tr.} = 1.212$ (P. 62) and also that the axial loading controls size (P. 65). If we had sized on the basis of transverse load, we would get a slightly smaller bearing:

(71) $$(r_o)_{tr.\ sizing} = (D_{tr.})\ (r_o)_{ref.tr.}$$

(72) $$= D_{tr} \left[\frac{P_{tr.\ shaft}}{\pi (q_o)_{des.tr.}} \right]^{1/2}$$

Using the numerical values of P. 64 gives

$$(r_o)_{tr.sizing} = (1.212)\left[\frac{8.87}{(3.14)(242,000)}\right]^{1/2} = (1.212)(.00342)$$
$$= .00415 \text{ in.}$$

$$(d_o)_{tr.\ sizing} = .0083 \text{ in.}$$

For axial load sizing (See PP. 11 and 25):

$$d_o = D(d_o)_{ref.}$$
$$= (1.225)(.0092) = .01126$$

The friction radius for transverse sizing is

$$(r_{fr.})_{tr.\ sizing} = \Delta_{tr.}\frac{\pi}{2}(r_o)_{ref.tr.} = (.964)(1.571)(.00342)$$

$$r_{fr.tr.\ sizing} = .00518 \text{ in.}$$

and (Eq. 74)

$$T_{fr.tr.\ 2\ brg.} = \mu\ (P_{tr})_{2brg.}\ (r_{fr})_{tr.}$$
$$= (.17)(8.87)(.00518)$$

$$T_{fr.tr.\ 2\ brg.} = .0106 \text{ lb. in.}$$

Comparing this to (2)(.0120) = .0240 in. lb. on P. 95 shows some theoretical advantage to the hemispherical conforming bearing over the cylindrical journal bearing.

Cases 7 and 8 TORROIDAL BEARINGS

Using the notation of the sketch (Figure 11) on P. 26 we have, corresponding to Equations 11, 12, and 57 (Φ is the longitude angle as on P. 54):

(78) $$q(\theta,\Phi) = q_o \frac{\sin\theta}{\sin\alpha} \cos\Phi \quad (0 \le \theta \le \alpha) \quad \left(-\frac{\pi}{2} \le \Phi \le \frac{\pi}{2}\right)$$

(21) $$r = r_1 + R\sin\theta$$

and

(22) $$r_o = r_1 + R\sin\alpha$$

The differential element of area dA is

(79) $$dA = (Rd\theta)(rd\Phi) = (Rd\theta)(r_1 + R\sin\theta)\, d\Phi$$

The friction torque due to the normal pressure $q(\theta,\Phi)$ on the area dA is

(80) $$dT_{fr}(\theta,\Phi) = \mu\, dNr = \mu q(\theta,\Phi)\, dA(\theta,\Phi) r(\theta)$$

which, when the equations above are used, can be written as

$$dT_{fr}(\theta,\Phi) = \mu q_o \frac{\sin\theta}{\sin\alpha} \cos\Phi\, (Rd\theta)(r_1 + R\sin\theta)$$

$$(d\Phi)(r_1 + R\sin\theta)$$

or as

(81)
$$dT_{fr} = \frac{\mu q_o r_o^3(1 - \frac{1}{\beta})}{\sin^4 \alpha} \Big[\frac{\sin^2\alpha}{\beta^2} \sin\theta$$

$$+ \frac{2}{\beta}(1 - \frac{1}{\beta}) \sin\alpha \sin^2\theta$$

$$+ (1 - \frac{1}{\beta})^2 \sin^3\theta \Big] (\cos\phi) d\phi \, d\theta$$

The friction torque then becomes

$$T_{fr} = \int_{\theta=0}^{\theta=\alpha} \int_{\phi = -\frac{\pi}{2}}^{\phi = \frac{\pi}{2}} dT_{fr} (\theta, \phi)$$

or

(82)
$$T_{fr}(q_o, \beta, \alpha) = \frac{2\mu q_o r_o^3 (1 - \frac{1}{\beta})}{\sin^4 \alpha} \Big[\frac{\sin^2\alpha}{\beta^2}(1 - \cos\alpha)$$

$$+ \frac{2 \sin\alpha}{\beta} (1 - \frac{1}{\beta})(\frac{\alpha}{2} - \frac{\sin 2\alpha}{4})$$

$$+ (1 - \frac{1}{\beta})^2 (\frac{2}{3} - \frac{2}{3} \cos\alpha - \frac{\cos\alpha \sin^2\alpha}{3}) \Big]$$

The Y_n component of the transverse load is zero because of the symmetry of $q(\theta, \phi)$ about the x axis ($\phi = 0$). The X_n component is given by

(83) $$-X_n = \int_{\theta=0}^{\theta=\alpha} \int_{\phi=-\frac{\pi}{2}}^{\phi=\frac{\pi}{2}} [q(\theta,\phi)\ dA](\sin\theta)(\cos\phi)$$

which, upon integration becomes

(84) $$-X_n = \frac{\pi\, q_o\, r_o^2\,(1-\frac{1}{\beta})}{2\ \sin^3\alpha}\left[\frac{\sin\alpha}{\beta}\left(\frac{\alpha}{2}-\frac{\sin 2\alpha}{4}\right) + \left(1-\frac{1}{\beta}\right)\left(\frac{2}{3}-\frac{2}{3}\cos\alpha-\frac{1}{3}\cos\alpha\ \sin^2\alpha\right)\right]$$

The symmetry of $q(\theta,\phi)$ about the x axis gives zero X_{fr} component of the friction force. The Y_{fr} component is given by

(85) $$-Y_{fr} = \int_{\theta=0}^{\theta=\alpha} \int_{\phi=-\frac{\pi}{2}}^{\phi=\frac{\pi}{2}} \mu[q(\theta,\phi)\ dA]\ \cos\phi$$

which upon integration becomes

(86) $$-Y_{fr} = \frac{\pi\mu q_o r_o^2(1-\frac{1}{\beta})}{2\sin^3\alpha}\left[\frac{\sin\alpha}{\beta}(1-\cos\alpha) + \left(1-\frac{1}{\beta}\right)\left(\frac{\alpha}{2}-\frac{\sin 2\alpha}{4}\right)\right]$$

The equilibrium equations, 66 and 67, then give

(87) $$P_{tr.\,1\,brg.} = \frac{\pi q_o r_o^2 \left(1 - \frac{1}{\beta}\right)}{2\sin^3 \alpha} \left[E^2(\alpha, \beta) + \mu^2 F^2(\alpha, \beta) \right]^{1/2}$$

and

(88) $$\tan\gamma = \frac{\mu F}{E}$$

where E and F are defined by

(89) $$E(\alpha, \beta) = \left[\frac{\sin\alpha}{\beta} \left(\frac{\alpha}{2} - \frac{\sin 2\alpha}{4}\right) + \left(1 - \frac{1}{\beta}\right)\left(\frac{2}{3} - \frac{2}{3}\cos\alpha - \frac{1}{3}\cos\alpha \sin^2\alpha\right) \right]$$

and

(90) $$F(\alpha, \beta) = \left[\frac{\sin\alpha}{\beta} (1 - \cos\alpha) + \left(1 - \frac{1}{\beta}\right)\left(\frac{\alpha}{2} - \frac{\sin 2\alpha}{4}\right) \right]$$

Using the definitions of D_{tr} and Δ_{tr} and the results above gives

(91) $$D_{tr} = \left[\frac{\sin^3\alpha}{\left(1 - \frac{1}{\beta}\right) \left(E^2 + \mu^2 F^2\right)^{1/2}} \right]^{1/2}$$

and

(92) $$\Delta_{tr} = \frac{8}{\pi^2 \sin\alpha} \left[\frac{(1 - \frac{1}{\beta}) E + \frac{\sin\alpha}{\beta} F}{(E^2 + \mu^2 F^2)^{1/2}} \right] (D_{tr})$$

As a partial check note that as β approaches ∞ the right side of 92 approaches the right side of 77 (for $\alpha_1 = 0$) and the right side of 92 approaches the right side of 73 for $\alpha_1 = 0$). Thus the limiting behavior as the torroidal bearing becomes a solid spherical bearing checks.

For numerical values note that for $\beta = \infty$ we get the same results as for the spherical bearing. Thus consider the two cases

$\alpha = 90^\circ$, $\beta = 5/3$ and $\alpha = 30^\circ$, $\beta = 5/3$

<u>$\alpha = 90^\circ$, $\beta = 5/3$</u>

(89) $$E(90^\circ, \tfrac{5}{3}) = \left[\tfrac{3}{5} (\tfrac{\pi}{4} - \tfrac{\sin 180^\circ}{4}) + (1 - .6)(\tfrac{2}{3} \cos 90^\circ - \tfrac{1}{3} \cos 90^\circ \sin^2 90^\circ) \right]$$

$$= .738$$

(90) $$F(90^\circ, \tfrac{5}{3}) = \left[(.6)(1 - 0) + (.4)(\tfrac{\pi}{4}) \right]$$

$$= .914$$

$(\mu = .17)$

(91) $$D_{tr} = \left[\frac{(1)^3}{(.4)\left[.738^2 + (.17)^2(.914)^2\right]^{1/2}} \right]^{1/2}$$

$$= 1.822$$

As we should expect, the cut off spherical bearing resists transverse load more efficiently (p. 62, $D_{tr} = 1.250$), because its inner edge makes a greater angle (36.8° in this case) to the transverse load than does that of the torroidal bearing (0° in all cases).

(92) $$\Delta_{tr} = \frac{8}{\pi^2(1)} \left[\frac{(.4)\ (.738) + (.6)\ (.914)}{.754} \right] (1.822)$$

$$= 1.651$$

Comparing this to $\Delta_{tr} = .998$ (P.66) for the hollow spherical bearing with the same α and β, shows that for the same load and stress the torroidal has more friction primarily due to its greater size.

$\alpha = 30^\circ, \quad \beta = \frac{5}{3}$

$$E(30^\circ, 1.667) = .0205$$

$$F(30^\circ, 1.667) = .0584$$

$$(E^2 + \mu^2F^2)^{1/2} = .0228$$

$$D_{tr} = \left[\frac{(.5)^3}{(.4)(.0228)} \right]^{1/2} = 3.70$$

$$\Delta_{tr} = \frac{8}{\pi^2 (.5)} \left[\frac{(.4)(.0205) + (.3)(.0584)}{.0228} \right] 3.70$$

$$= 6.75$$

Again the torroidal bearing is less efficient in resisting transverse loads ($D_{tr.sph.} = 2.71$, (P. 64)) and for the same loads and stresses has a greater friction radius ($\Delta_{tr.sph.} = 4.09$ (P. 67)).

<u>Case 9</u> <u>CONICAL BEARING</u>

For this case we assume the normal pressure distribution (See sketch Fig. 12 (P. 29)):

(93) $$q(r,\phi) = q_o \cos\phi \qquad (r_i \leq r \leq r_o)$$

$$\left(-\frac{\pi}{2} \leq \phi \leq \frac{\pi}{2}\right)$$

The differential element of area is

(94) $$dA = \left(\frac{dr}{\cos\nu}\right)(r\, d\phi)$$

The friction torque due to the normal pressure $q(r,\phi)$ on the area dA is

(95) $$dT_{fr}(r,\phi) = \mu\, dN\, r = \mu q(\phi) dA(r,\phi) r$$

or

(96) $$dT_{fr}(r,\phi) = \mu\, q_o (\cos\phi) \left(\frac{r\, dr\, d\phi}{\cos\nu}\right)(r)$$

The total friction torque is then

$$T_{fr.\,1\,brg.} = \int_{r=r_1}^{r=r_o} \int_{\phi = -\frac{\pi}{2}}^{\phi = \frac{\pi}{2}} \frac{\mu\, q_o \cos\phi\, r^2\, dr d\phi}{\cos\nu}$$

or

(97) $$T_{fr.\,1\,brg.} = \frac{2\mu\, q_o\, r_o^{\,3}}{3\cos\nu}\left(1 - \frac{1}{\beta^3}\right)$$

The Y_n component of the transverse load is again zero by symmetry and the X_n component is given by

$$-X_n = \int_{r=r_1}^{r=r_o} \int_{\phi = -\frac{\pi}{2}}^{\phi = \frac{\pi}{2}} q(\phi)\, dA \sin\nu \cos\phi$$

which upon integration becomes

(98) $$-X_n = \frac{\pi q_o r_o^{\,2} \tan\nu}{4}\left(1 - \frac{1}{\beta^2}\right)$$

The X_{fr} component of the friction force is again zero by symmetry while the Y_{fr} component is given by

$$-Y_{fr} = \int_{r=r_1}^{r=r_o} \int_{\phi = -\frac{\pi}{2}}^{\phi = \frac{\pi}{2}} \mu\, q(\phi)\, dA \cos\phi$$

which upon integration becomes

$$(99) \qquad -Y_{fr} = \frac{\mu\, q_o \pi r_o^2}{4 \cos\nu}\left(1 - \frac{1}{\beta^2}\right)$$

The equilibrium equations 66 and 67 give

$$(100) \qquad P_{tr.\ 1\ brg.} = \frac{\pi q_o r_o^2}{4 \cos\nu}\left(1 - \frac{1}{\beta^2}\right)\left(\sin^2\nu + \mu^2\right)^{1/2}$$

and

$$(101) \qquad \tan\gamma = \frac{\mu}{\sin\nu}$$

Using the definitions of D_{tr} and Δ_{tr} with the above results gives

$$(102) \qquad D_{tr} = \left[\frac{2 \cos\nu}{\left(1 - \frac{1}{\beta^2}\right)\left(\sin^2\nu + \mu^2\right)^{1/2}}\right]^{1/2}$$

and

$$(103) \qquad \Delta_{tr} = \frac{16}{3\pi^2}\,\frac{\left(1 - \frac{1}{\beta^3}\right)\left(D_{tr}\right)}{\left(1 - \frac{1}{\beta^2}\right)\left(\sin^2\nu + \mu^2\right)^{1/2}}$$

For numerical values use $\nu = 45^\circ$, and $\beta = \frac{5}{3}$, taking $\mu = .17$ as usual; then

$$D_{tr} = \left[\frac{(2)\ (\cos 45^o)}{(1 - .6^2)\ [(.707)^2 + (.17)^2]^{1/2}} \right]^{1/2}$$

$$= \underline{1.745}$$

and

$$\Delta_{tr} = \frac{16\ \ (1 - .6^3)\ (1.745)}{3\pi^2\ (1 - .6^2)\ (.727)}$$

$$= 1.581$$

These seem in line with the other numerical values.

<u>Case 10</u> <u>Bearing with Theoretical Line Contact</u> Using Figure 13 of P. 31 and the longitude angle ϕ, we assume a transverse normal force distribution of

(104) $$p(\phi) = p_m \cos\phi \quad \frac{\text{lb.}}{\text{in. of cir.}} \qquad \left(-\frac{\pi}{2} \leq \phi \leq \frac{\pi}{2} \right)$$

The arc length on which this acts is

(105) $$ds = r_o\ d\phi$$

so that the differential friction torque becomes

$$dT_{fr} = \mu p(\phi)\ (ds)(r_o) = (\mu\ p_m)(\cos\phi)(r_o)(d\phi)(r_o)$$

The total friction torque is then

$$(106) \qquad T_{fr} = \int_{\phi = -\frac{\pi}{2}}^{\phi = \frac{\pi}{2}} dT_{fr} = 2\mu p_m r_o^2$$

The X_n component of transverse force is given by

$$- X_n = \int_{\phi = -\frac{\pi}{2}}^{\phi = \frac{\pi}{2}} (p_m \cos\phi)(r_o \, d\phi)(\sin\nu)(\cos\phi)$$

or

$$(107) \qquad - X_n = \frac{\pi}{2} (p_m r_o \sin\nu)$$

The Y_{fr} component of transverse force is given by

$$- Y_{fr} = \int_{-\frac{\pi}{2}}^{\frac{\pi}{2}} \mu (p_m \cos\phi)(r_o \, d\phi)(\cos\phi)$$

or

$$(108) \qquad - Y_{fr} = \frac{\mu \pi p_m r_o}{2}$$

The equilibrium equations 66 and 67 then give

$$(109) \qquad P_{tr.1\ brg.} = \frac{\pi}{2} p_m r_o (\sin^2\nu + \mu^2)^{1/2}$$

and

(110) $\tan\gamma = \frac{\mu}{\sin\nu}$

Using the definitions of D_{tr} and Δ_{tr} with the results above gives

(111) $$D_{tr} = \left[\frac{r_o \, q_o}{p_m \, (\sin^2\nu + \mu^2)^{1/2}} \right]^{1/2}$$

and

(112) $$\Delta_{tr} = \frac{8 \, (D_{tr})}{\pi^2 \, (\sin^2\nu + \mu^2)^{1/2}}$$

Eliminating a between equations 124 and 125 gives

(113) $$p_m = \frac{\pi \, R_o q_o^{\,2}}{Eo}$$

Using the last equation to eliminate p_m from the expression above for D_{tr} gives

(114) $$D_{tr} = \left[\frac{1}{\pi} \frac{E_o}{q_o} \frac{r_o}{R_o} \frac{1}{(\sin^2\nu + \mu^2)^{1/2}} \right]^{1/2}$$

If r_o has been determined with axial load sizing, Equations 4, 5, and 29 give

(115) $$r_o \text{ axial load sizing} = \frac{P_{axial}\, E_o}{2\pi^2 \left((q_o)_{axial}\right)^2 R_o \cos\nu}$$

while with radial load sizing equations 109, 124, and 125 give

(116) $$(r_o)_{\substack{\text{transverse}\\ \text{load sizing}}} = \frac{(2\, P_{tr.1\ brg.})\, E_o}{\pi^2\, q_o^2\, R_o\, (\sin^2\nu + \mu^2)^{1/2}}$$

To determine whether sizing is controlled by axial or transverse loading we take the ratio of $(r_o)_{axial\ load\ sizing}$ over $(r_o)_{tr.\ load\ sizing}$ and see whether it is greater than one or less than one. Thus

(117) $$\frac{(r_o)_{\substack{\text{axial load}\\ \text{sizing}}}}{(r_o)_{\substack{\text{transverse}\\ \text{load sizing}}}} = \left(\frac{P_{axial}}{P_{tr.2\ brg.}}\right)\left(\frac{\left((q_o)_{tr.\ design}\right)^2}{\left((q_o)_{axial\ design}\right)^2}\right)\left[\frac{(\sin^2\nu + \mu^2)^{1/2}}{2\cos\nu}\right]$$

If this ratio is set equal to one we can solve for an "optimum" angle ν for this type of bearing, in the sense that the bearing has equal strength in both directions. This does not necessarily give the lowest friction torque, or the best angle ν from a wedging point of view however, and should be used with caution.

To see what happens let us take a particular numerical case. Taking

$$P_{axial} = 15.95 \text{ lb. (P. 114)}$$

$$P_{tr.2\ brg.} = 8.87 \text{ lb. (P. 124)}$$

using the same design pressure q_o for axial loading and transverse loading, and setting the left hand side of Eq. 117 equal to one gives

$$1 = \left(\frac{15.95}{8.87} \right) \left(\frac{1}{2}\right) \frac{(\sin^2\nu + \mu^2)^{1/2}}{\cos\nu}$$

For $\mu = .17$, we get $\nu = 47.4^\circ$ which is so close to 45° that we can consider ν to have been 45° and axial load sizing to have controlled. Equation (111) then gives

$$\Delta_{tr} = \frac{8(D_{tr})}{\pi^2 (\sin^2 45^\circ + 17^2)^{1/2}} = 1.112 \ (D_{tr})$$

Using the data of PP. 34, 35 in Equation (114) gives

$$D_{tr} = \left[\frac{(21 \times 10^6)(.0144)}{(3.14)(285{,}000)(.0203)(.707^2 + .17^2)^{1/2}} \right]^{1/2}$$

$$D_{tr} = 4.72$$

and

$$\Delta_{tr} = 1.112(4.72) = 5.25$$

which are in line with these quantities for the other bearings considered.

SECTION III

JOURNAL BEARINGS

Having rejected vee jewel bearings on the basis of their transverse flexibility (see SECTION IV), we are left with two general types of bearings; journal bearings, and combined thrust and transverse bearings. The possibility of the use of a journal bearing for the forward bearing, and in conjunction with a thrust bearing for the aft bearing will now be considered.

A cross sectional view of a journal bearing is shown in Fig. 17.

A cylindrical shaft of diameter d_s(in.) turns in part of a torroidal jewel with inside diameter $d_s + c$ (in.) and meridian radius R_B (in.). As a limiting case the bearing may be cylindrical ($R_B = \infty$) and the axial clearance shown may not exist or may be replaced by some provision for withstanding a small thrust load. (Bearings with appreciable thrust capabilities are treated separately in SECTIONS I and II.)

Contact Stress Analysis

The limitations on d_s, R_B, and $P_{tr.1\ brg.}$ that are imposed by contact stress considerations will be considered first.

When two convex bodies with finite principal radii of curvature R_1, R_1', R_2 and R_2' are brought into contact, the locus of all points on the surfaces that are initially the same small distance z apart, measured normal to the common tangent plane, is the elliptical curve with the equation

FIGURE XVII

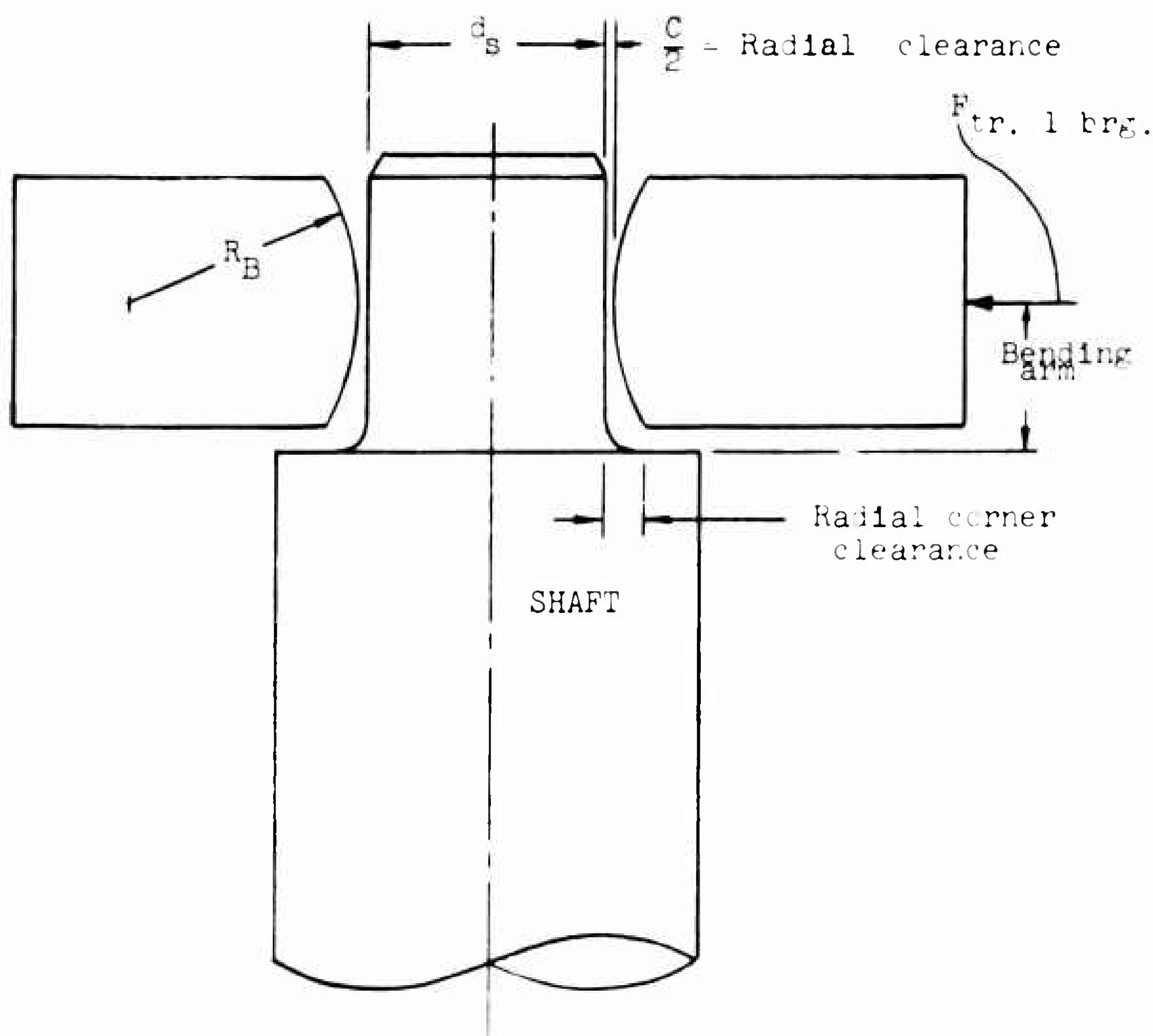

TYPICAL JOURNAL BEARING

AND NOMENCLATURE

(118) $$z = Ax^2 + By^2$$

where x and y are cartesian coordinates in the tangent plane, A and B are given by the solution of

(119) $$A + B = \frac{1}{2}\left(\frac{1}{R_1} + \frac{1}{R_1'} + \frac{1}{R_2} + \frac{1}{R_2'}\right)$$

and

(120) $$B - A = \frac{1}{2}\left[\left(\frac{1}{R_1} - \frac{1}{R_1'}\right)^2 + 2\left(\frac{1}{R_1} - \frac{1}{R_1'}\right)\left(\frac{1}{R_2} - \frac{1}{R_2'}\right)\cos 2\psi + \left(\frac{1}{R_2} - \frac{1}{R_2'}\right)^2\right]^{1/2}$$

and where ψ is the angle between the normal planes containing $\frac{1}{R_1}$ and $\frac{1}{R_2}$. (See for example Timoshenko and Goodier, <u>Theory of Elasticity</u> pp. 377-382.)

When the bodies are pressed together, the boundary of the contact area is a small ellipse with major and minor axes determined by the force, the elastic constants of the materials, and by the quantity θ where

(121) $$\cos\theta = \frac{B - A}{B + A}$$

The Hertz contact stress theory will not be valid unless the major and minor axes of the ellipse of contact are small compared to the smallest of R_1, R_1', R_2, and R_2'.

For the case of two long cylinders with parallel axes $\psi = 0$, $R_1' = \infty$, $R_2' = \infty$, the ellipse (118) becomes two parallel lines, $(B - A)$ becomes equal to $(B + A)$, θ is zero, and the surface of contact becomes a rectangle of long finite length and short width compared to R_1 and R_2. If the end effects are neglected and the applied load is uniformly distributed along the length, a valid limiting solution (for $\theta \to 0$) is obtained. However, in general, as θ approaches zero, the two surfaces become more and more nearly conforming in at least one direction, the major axis of the ellipse of contact becomes large compared to the smallest radius of curvature, and the contact stress theory becomes invalid. Thus the case of two long cylinders with parallel axes and load uniformly distributed along their length becomes the only valid limiting case of contact stress theory as θ approaches zero.

For the bearing under consideration we have the two surfaces conforming in the circumferential direction for approximately half the circumference but we <u>do not have a uniform distribution of load along this common element</u>. The end effects are gradual however, since the conforming surfaces turn smoothly with respect to the direction of the applied force. (With a roller of finite length pressed onto another the end effects are not negligible and the solution is only valid away from the ends.)

To show the conformity of the surfaces take

$$R_1 = \frac{d_s}{2}$$

Then, (see Figure 18)

$$R_1' = \infty$$

$$R_2 = -\left(\frac{d_s}{2} + \frac{c}{2}\right)$$

$$R_2' = R_B$$

$$\psi = 0$$

and

$$A + B = \frac{1}{2}\left(\frac{1}{R_1} + \frac{1}{R_1'} + \frac{1}{R_2} + \frac{1}{R_2'}\right)$$

$$= \frac{1}{2}\left(\frac{2}{d_s} + \frac{1}{\infty} - \frac{2}{d_s + c} + \frac{1}{R_B}\right)$$

$$= \frac{c}{d_s(d_s + c)} + \frac{1}{2\,R_B}$$

$$B - A = \frac{1}{2}\left[\left(\frac{1}{R_1} - \frac{1}{R_1'}\right)^2 + 2\left(\frac{1}{R_1} - \frac{1}{R_1'}\right)\left(\frac{1}{R_2} - \frac{1}{R_2'}\right)\cos 2\psi + \left(\frac{1}{R_2} - \frac{1}{R_2'}\right)^2\right]^{1/2}$$

FIGURE XVIII

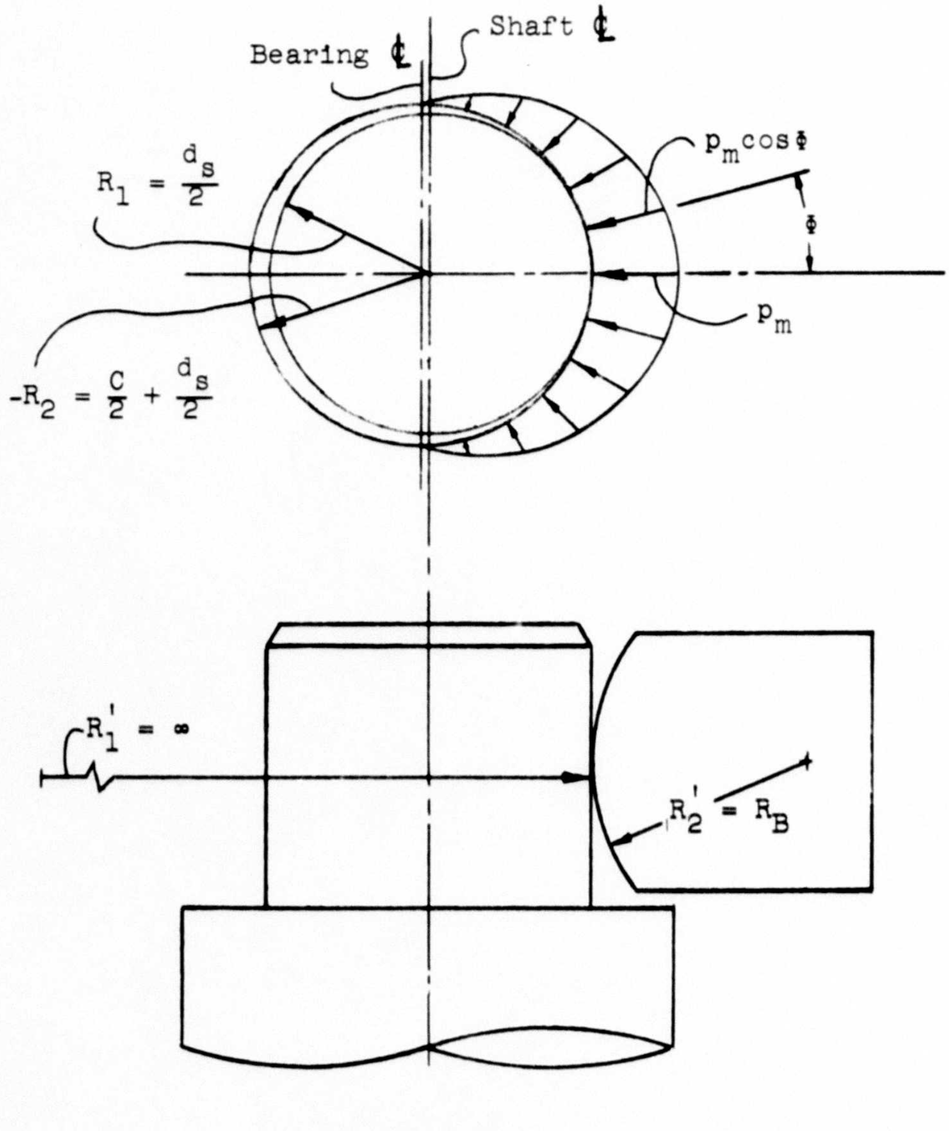

JOURNAL BEARING UNDER

APPLIED LOAD

$$= \frac{1}{2}\left[\left(\frac{2}{d_s} - \frac{1}{\infty}\right)^2 + 2\left(\frac{2}{d_s}\right)\left(- \frac{2}{d_s + c} - \frac{1}{R_B}\right)(1)\right.$$

$$\left. + \left(- \frac{2}{d_s + c} - \frac{1}{R_B}\right)^2\right]^{1/2}$$

$$= \pm \frac{1}{2}\left[\left(\frac{2}{d_s}\right) + \left(- \frac{2}{d_s + c} - \frac{1}{R_B}\right)\right]$$

$$= \pm \left[\frac{c}{d_s(d_s + c)} - \frac{1}{2R_B}\right]$$

$$\cos\theta = \frac{B - A}{B + A} = \frac{\pm\left[\frac{c}{d_s(d_s + c)} - \frac{1}{2R_B}\right]}{\left[\frac{c}{d_s(d_s + c)} + \frac{1}{2R_B}\right]}$$

If R_B is very large the two surfaces conform in two directions. If not, $\frac{c/d_s}{d_s + c}$ is negligible in comparison to $\frac{1}{2R_B}$ and $\cos\theta = \mp 1$. The minus sign has no significance and so θ approaches zero in this case for the small radial clearances required in a precision mechanism of this type.

For an approximate solution we procede as follows. The conforming direction is the circumferential one. We assume, as an approximation to the pressure distribution in this direction, a cosine variation with angle. Thus (see Figure 18)

(122) $$p(\Phi) = p_m \cos\Phi$$

Since the resultant of this distributed load must equal $P_{\text{transverse 1 brg.}}$ we have

$$P_{\text{tr.1 brg.}} = \int_{\Phi = -\frac{\pi}{2}}^{\Phi = \frac{\pi}{2}} (p_m \cos\Phi)(\frac{d_s}{2}\, d\Phi) \cos\Phi = p_m \frac{d_s}{2} \frac{\pi}{2}$$

or

(123) $$p_m = \frac{4(P_{\text{tr. 1 brg.}})}{\pi\, d_s}$$

Next we compute the maximum contact pressure q_o $(\frac{\text{lb.}}{\text{in.}})$ between two cylinders with curvatures in planes normal to their conforming direction of $\frac{1}{R_1'} = \frac{1}{\infty}$ and $\frac{1}{R_2'} = \frac{1}{R_B}$ which are pressed together by a <u>uniform</u> force per unit length in their conforming direction of p_m $(\frac{\text{lb.}}{\text{in.}})$. This gives

(124) $$q_o = \frac{2\, p_m}{\pi\, a}$$

where a is the (small) half width of the (deformed) rectangle of contact and is given by

(125) $$a = \left[\frac{4\, p_m\, R_o'}{\pi\, E_o} \right]^{1/2}$$

and

$$(126) \qquad \frac{1}{R_c} = \frac{1}{R_1} + \frac{1}{R_2}$$

while E_o is computed from Equation 131 Page 101, SECTION IV. (See for example Timoshenko and Goodier, PP. 381-2.)

Finally we consider that the value of q_o calculated in this manner for an equivalent cylinder of curvature $\frac{1}{R_B}$ pressed onto a plane of curvature $\frac{1}{\infty} = 0$ by a uniform load per unit length of p_m calculated from $P_{tr. 1\ brg.}$ and d_s as above) is a good approximation to the maximum value of contact pressure q_o that actually exists. Because of the smooth variation of p with ϕ and the reasonableness of the assumed cosine distribution, the writer feels that this solution will give results of ordinary engineering accuracy, i.e., no greater error will be introduced than that due to tolerances on R_B or estimates of $E_{bearing}$ for example.

Equations 123, 124, and 125 can be combined to give an expression for the minimum value $R_{B\ min.}$ (or $R_{o\ min.}$ if we want to allow for the possibility of the shaft having non zero meridian curvature) in terms of the transverse load, $P_{tr. 1\ brg.}$ and the material properties. This gives

$$(127) \qquad R_{o\ minimum} = \frac{4}{\pi^2} \frac{E_o\ P_{tr. 1\ brg.}}{q_o^2\ d_s}$$

The differential friction torque, $dT_{fr.}$, is

$$dT_{fr} = (p_m \cos\phi\, \mu)(\frac{d_s}{2})$$

Summing up all these differential torques from $\phi = -\frac{\pi}{2}$ to $\phi = \frac{\pi}{2}$, and using Eq. 123 to eliminate p_m gives

$$(128) \qquad T_{fr.\,1\,brg.} = \int_{-\frac{\pi}{2}}^{\frac{\pi}{2}} p_m (\frac{d_s}{2})^2 \mu \cos\phi \, d\phi$$

$$= \mu P_{tr.\,1\,brg.} (\frac{d_s}{2})(\frac{4}{\pi})$$

In this analysis the meridian section of the bearing has been assumed to be convex with R_B as its radius of curvature. This effectively gives the shaft a simple support, i.e., one not capable of applying an end moment. If R_B is increased so that the shaft and bearing conform in the axial direction also, then the bearing is capable of exerting an end moment on the shaft, and for a given d_s the shaft becomes stiffer. While this increase in stiffness is an advantage, it would be balanced out by two disadvantages:

1. Instead of theoretical line contact in the undeformed state and contact over an area with one small dimension in the deformed state, there is theoretical area contact. The usual effect of this is to increase the number of small sur-

face irregularities that are elastically (say) pushed out of the way each revolution and to thus increase the coefficient of friction.

2. When the bearing is exerting a bending moment on the shaft in addition to a net transverse load, the normal forces producing friction are larger than the net transverse load by twice the quotient of restraining moment over effective bearing length. Thus in Figure 19 the normal forces on the shaft, which produce friction, are increased from $P_{tr.\ 1\ brg.}$ for the simple support to $P_{tr.\ 1\ brg.} + \frac{2\ M_{rest.}}{L_{eff}}$ for the restrained support.

Thus if a journal bearing is used, there should be theoretical line contact in the unloaded state (simple support).

Equation 128 shows that the smallest shaft diameter possible gives minimum friction. The lower limit on shaft diameter for this application is about $d_{s\ min.} = .020$ in. (Anything less would not be stiff enough.) For a transverse load on one bearing of $P_{tr.\ 1\ brg.} = 4.43$ lb. (see Page 124) this gives an average shear stress of

$$S_{s\ ave.} = \frac{P_{tr.\ 1\ brg.}}{.785\ d_s^2} = \frac{4.43}{(.785)(.020)^2} = 14{,}1000 \text{ psi}$$

For a bending arm (see Figure 17, P. 84) of one diameter the nominal bending stress at the fillet is

FIGURE XIX

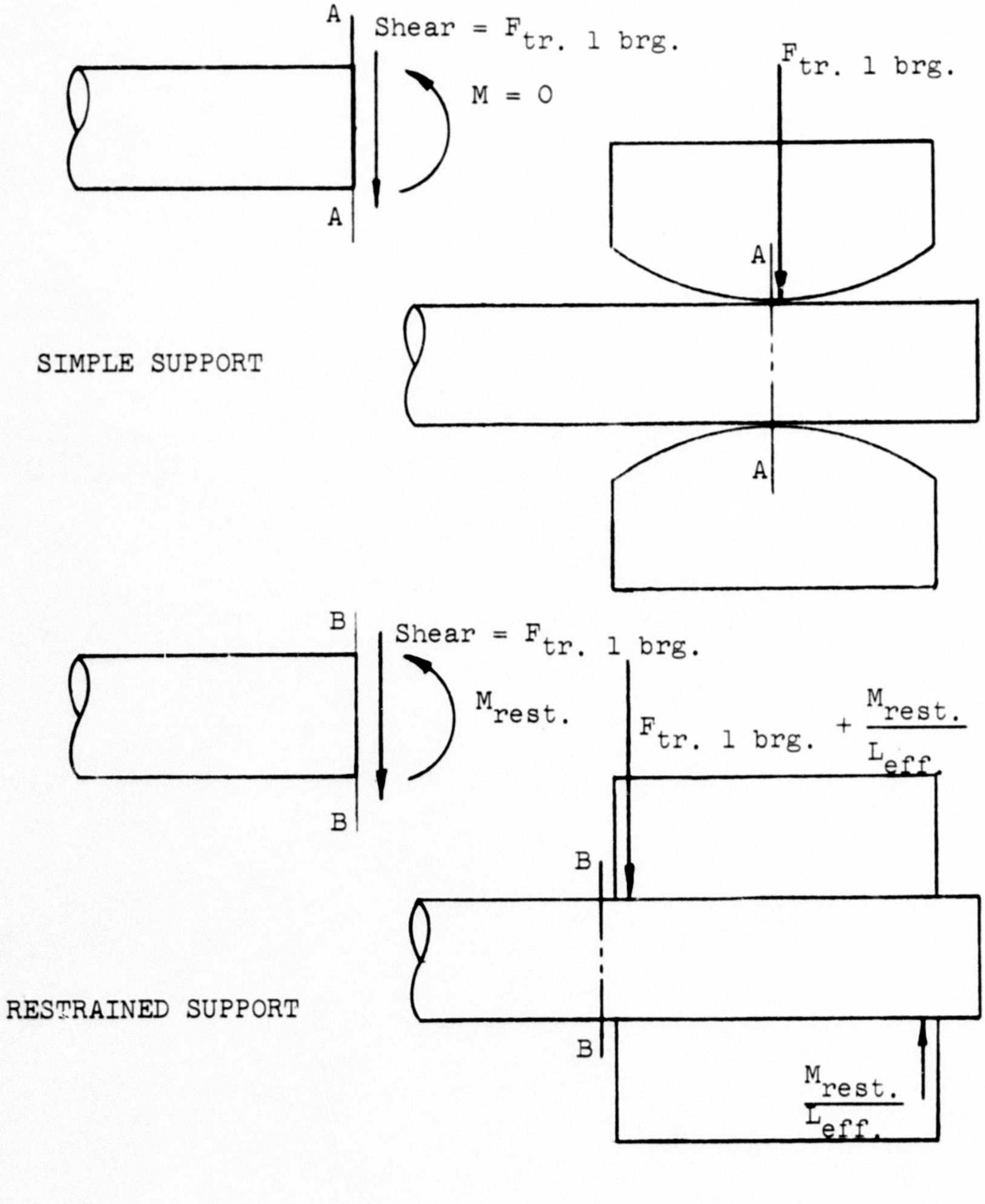

DIAGRAM SHOWING INCREASED NORMAL FORCES WHICH OCCUR WHEN A SHAFT SUPPORT CAN APPLY A BENDING MOMENT

$$S_{nom.\ bending} = \frac{32\ M}{\pi\ d_s^3} = \frac{(32)(4.43\ x\ .020)}{(3.14)(.020)^3} = 113{,}000\ psi$$

While this high nominal bending stress is not desirable, it is not completely out of the question either. However, we use

$$d_s = .025\ in.$$

in the calculations that follow, tentatively assuming that the increase in friction torque is more acceptable than the difficulties associated with the smaller shaft. Thus with typical values of

$P_{tr.\ 1\ brg.} = 4.43$ lb. (P. 124)

$d_s = .025$ in. (P. 95)

$q_o = (.85)(285{,}000) = 242{,}000$ psi (arbitrarily reduced 15% because of the larger nominal size, see pp. 108 and 134.)

$\mu = .17$ (P. 122)

we have

$$T_{fr.\ 1\ brg.\ typical} = \mu\ P_{tr.\ 1\ brg.}\ \left(\frac{d_s}{2}\right)\left(\frac{4}{\pi}\right)$$

$$= (.17)(4.43)\left(\frac{.025}{2}\right)\left(\frac{4}{3.14}\right)$$

$$= (.17)(4.43)(.01592)$$

$$= .0120\ in.\ lb.$$

This does not compare too unfavorably with the friction torque of a vee jewel bearing that is turning under its rated axial load (.00825 in. lb. on P. 123), but the present torque acts during the entire flight of the projectile.

(127) $$R_{o\ minimum} = \frac{4}{\pi^2}\,\frac{E_o\ P_{tr\ 1\ brg.}}{q_c^2\ d_s}$$

$$= \frac{(4)(21 \times 10^6)(4.43)}{(3.14)^2\ (242{,}000)^2\ (.025)}$$

(See P. 108 for E_o)

$$= .0258 \text{ in.}$$

Using a straight shaft gives

$$R_{B\ min.} = R_{o\ min.} = .0258 \text{ in.}$$

This is drawn approximately to scale in Figure 20 using a bearing length of 1.5 x d_s. The minimum radial corner clearance is then

$$\text{Min. Rad. Cor. Cl.} = R_{B\ min.}\left[1 - \cos\left(\sin^{-1}\frac{L/2}{R_{B\ min.}}\right)\right]$$

$$= .0258\left[1 - \cos\left(\sin^{-1}\frac{(.75)(.025)}{(.0258)}\right)\right]$$

FIGURE XX

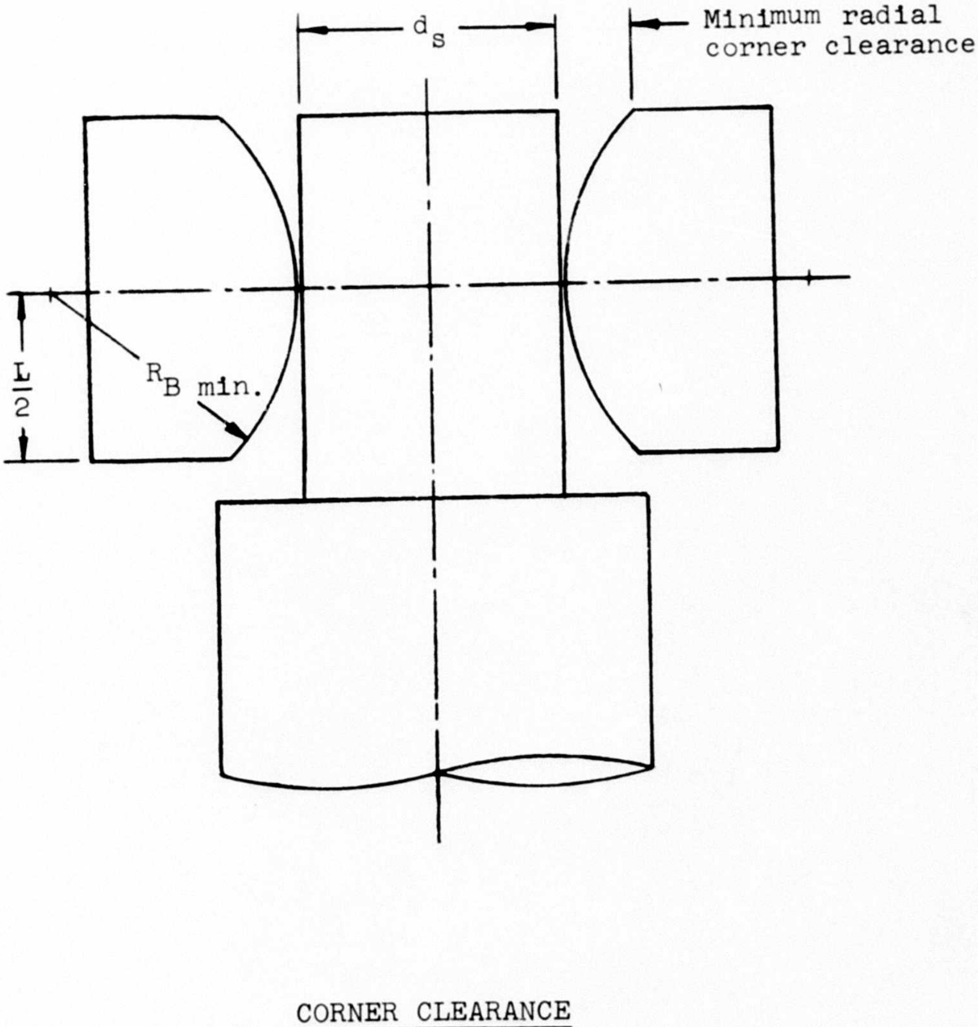

CORNER CLEARANCE

$$= .0258(.313)$$

$$= .00807 \text{ in.}$$

which is quite reasonable. The approximate half width of contact is

$$a = \left[\frac{4\, p_m\, R_o}{\pi\, E_o}\right]^{1/2} = \left[\frac{4}{\pi}\, \frac{R_o\, P_{tr.1\, org.}}{E_o\, d_s}\right]^{1/2}$$

$$a = \frac{4}{3.14}\left[\frac{(.0258)(4.43)}{(21 \times 10^6)(.025)}\right]^{1/2}$$

$$a = .000595 \text{ in.}$$

This compares to a = .00517 as the radius of the contact circle of a vee bearing under design axial load (P. 119). It is less than the other value because the other dimension of the area of contact is finite and about one-half the circumference. The advantage of a small value of a here is only in minimizing the required smoothness of contact surface, i.e., there is no reduction in friction radius with a as for a vee bearing.

SECTION IV

CONTACT STRESSES IN CONVENTIONAL VEE JEWEL BEARINGS IN INSTRUMENTS AND IN THE PROPOSED APPLICATION

A. Analysis of Contact Stresses in a Vee Jewel Bearing

Consider the vee pivot and jewel shown in Figure 21. Let:

P = force pushing them together (lb.)

R_1 = bearing radius, assumed spherical (in.)

R_2 = pivot tip radius, assumed spherical (in.)

E_1 = bearing modulus of elasticity (psi)

E_2 = shaft modulus of elasticity (psi)

The stresses will be calculated using Hertz contact stress theory for two spherical bodies. (See Timoshenko and Goodier, Theory of Elasticity, PP. 372-377.)

The two spherical surfaces deform so that contact occurs over a circle of small radius.

Let:

a = radius of circle of contact (in.)

R_1, R_2 = radii of the balls, positive if convex (in.)

ν_1, ν_2 = Poisson's ratio for the two materials

Then (Equation 219 of reference)

FIGURE XXI

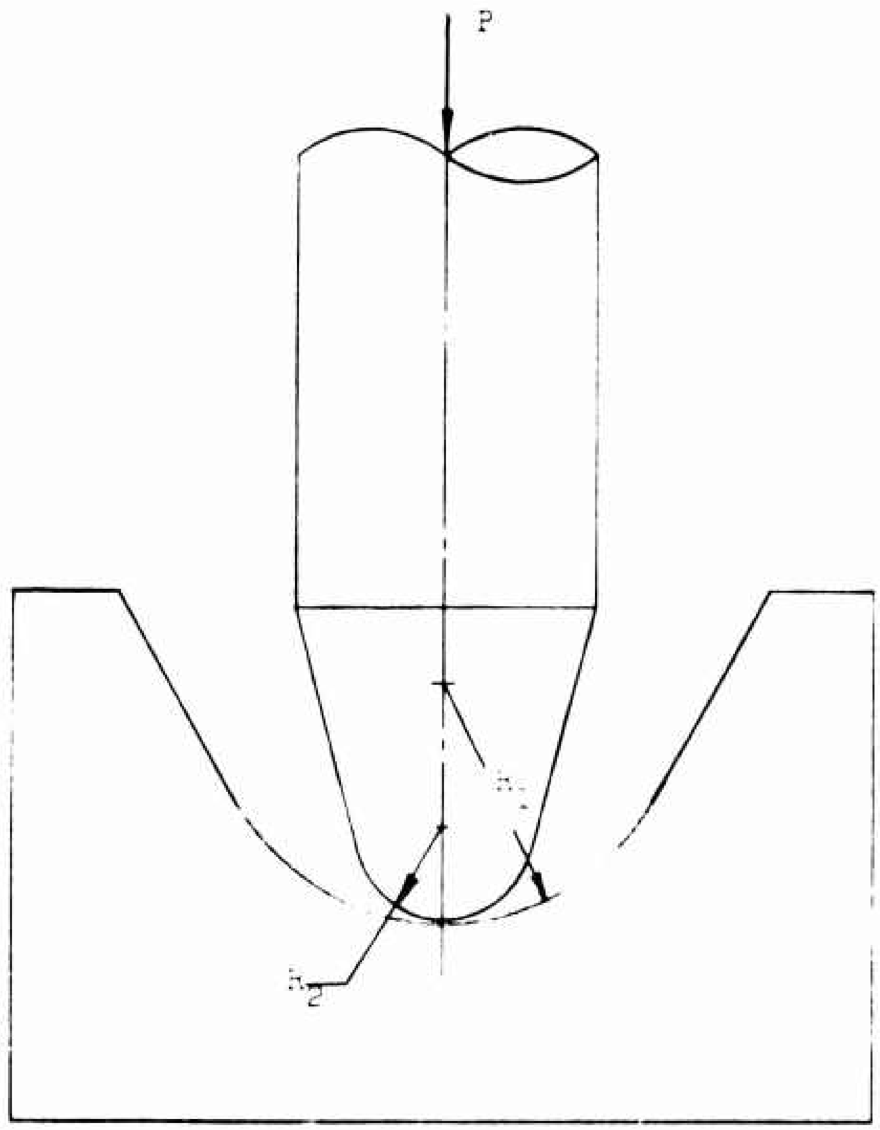

ANALYSIS OF CONTACT STRESSES

IN A VEE JEWEL BEARING

$$\text{(129)} \qquad a = \left\{ \frac{3\pi}{4} P \left[\frac{1 - \nu_1^2}{\pi E_1} + \frac{1 - \nu_2^2}{\pi E_2} \right] \left[\frac{1}{\frac{1}{R_1} + \frac{1}{R_2}} \right] \right\}^{1/3}$$

Defining R_o and E_o by

$$\text{(130)} \qquad \frac{1}{R_o} = \frac{1}{R_1} + \frac{1}{R_2}$$

and

$$\text{(131)} \qquad \frac{1}{E_o} = \frac{1 - \nu_1^2}{E_1} + \frac{1 - \nu_2^2}{E_2}$$

and substituting into Equation 129 gives

$$\text{(132)} \qquad a = \left\{ \frac{3P\, R_o}{4\, E_o} \right\}^{1/3}$$

The pressure distribution over the circle of contact is hemispherical with a maximum pressure at the center. Let

q_o = maximum pressure on contact area (psi).

Then (Equation 218 of reference)

$$\text{(133)} \qquad q_o = \frac{3P}{2\pi a^2}$$

Points remote from the contact area (say the centers of the balls or in this case the deflection of the gear with respect to the case due to pivot deformation) approach each other by α (inches) where (Eq. 219 of ref.) α is given by

$$(134) \qquad \alpha = \left\{ \frac{9\pi^2 P^2}{16} \; \frac{1}{(mE_o)^2} \; \frac{1}{R_o} \right\}^{1/3}$$

Using Eq. 132 gives

$$(135) \qquad \alpha = \frac{a^2}{R_o}$$

The maximum shear stress occurs at a depth below the surface of about .47a (See P. 376 of Timoshenko and Goodier or P. 41-2 of the <u>Handbook of Engineering Mechanics.</u>) and for Poisson's ratio of .3 for both materials is given by

$$(136) \qquad \tau_{max.} = .31\ q_o$$

where

$\tau_{max.}$ = maximum shear stress (psi.)

These formulas assume:

(1) That a is small compared to $|R_1|$ and $|R_2|$

(2) That the material remains elastic

In order to determine the allowable material properties (in particular $\tau_{max.}$) we consider loads and sizes that are the limits of conservative design practice.

The Richard H. Bird & Co., Inc., Catalog of Precision Jewel Bearings, states:

The glass jewel can be used successfully where the weight of the moving element is of the order of 750 milligrams or less. Sapphire jewels should be considered when the weight of the moving element exceeds this amount."

"Hard Glass -

Young's Modulus - 12.7 x 10^{-6} psi."
(obviously a misprint)

"Synthetic Sapphire -

Compressive Strength - 300,000 psi.

Maximum Bending Stress - 94,000 to 100,000 psi. Varies with angle of stress."

The dimensions of a typical standard glass vee jewel are:

"O.D. = .070 in.
Thickness = .040 in.
Angle = 80° (total included)
Depth of Vee = .012 - .018 in."

The Bird catalog also states "A radius ratio (jewel radius to pivot radius) of 2.5 or 3.0 to 1 is acceptable."

In addition the catalog of the Industrial Sapphire Co., Quakertown, Pa. lists:

"Synthetic Sapphire -
Compressive Strength - 300,000 psi. @ $77^\circ F$
Young's Modulus - 50 to 55 x 10^6 (dependent on position of crystal C-axis)
Modulus of Rupture -
$30^\circ C$ - 40 to 130,000 psi.
$540^\circ C$ - 23,000 to 50,000 psi."

The Bird catalog also lists as its standard sapphire vee jewel with the largest radius R_B:

"Part No. RB 303035
O.D. = .120 in.
Thickness = 0.125 in.
Angle = $110^\circ \pm 5^\circ$
Radius = .009/011 in.
Depth = .030/.035 in."

From this limited information we infer that the limits of typical practice are:

For Glass

$$E_1 = 12.7 \times 10^6 \text{ psi.}$$

$$P_{limiting} = 750 \text{ mg.} \times \frac{1}{4.54 \times 10^5} \frac{\text{lb.}}{\text{mg.}}$$

$$= .00165 \text{ lb.}$$

$$R_{1\ typical} = -\ .0040 \text{ in.}$$

$$R_{2\ typical} = .0015 \text{ in.}$$

(Take $\nu = .3$ and assume $E_2 = 30 \times 10^6$ psi.)

For Sapphire

$$q_{o\ limiting} = 300{,}000 \text{ psi.}$$

$$E_{1\ typical} = 52.5 \times 10^6 \text{ psi.}$$

$$R_{1\ typical} = -\ .010 \text{ in.}$$

$$R_{2\ typical} = .0035 \text{ in.}$$

(Take $\nu = .3$ and assume $E_2 = 30 \times 10^6$ psi.)

Using the formulas above gives:

For Glass

$$\frac{1}{R_o} = \frac{1}{R_1} + \frac{1}{R_2} = \frac{1}{.0015} + \frac{1}{-\ .0040} = 416.7 = \frac{1}{.00240}$$

$$\frac{1}{E_o} = \frac{1-\nu_1^2}{E_1} + \frac{1-\nu_2^2}{E_2} = (1-.3^2)\left[\frac{1}{30 \times 10^6} + \frac{1}{12.7 \times 10^6}\right]$$

$$= \frac{1}{9.79 \times 10^6}$$

$$a = \left[\frac{3P\,R_o}{4\,E_o}\right]^{1/3} = \left[\frac{(3)(.00165)(.00240)}{(4)(9.79 \times 10^6)}\right]^{1/3}$$

$$= \left[.303 \times 10^{-12}\right]^{1/3}$$

$$= .0000672 \text{ in.}$$

$$\frac{a}{R_2} = \frac{.0000672}{.0015} = \frac{.672}{15} = .0448 \quad \text{(which is small enough)}$$

$$\alpha = \frac{a^2}{R_o} = \frac{(.672 \times 10^{-4})^2}{2.4 \times 10^{-3}} = 1.88 \times 10^{-6} \text{ in.}$$

$$q_o \text{ limiting typical} = \frac{3P_{lim.}}{2\pi\,a^2} = \frac{(3)(.00165)}{(2)(3.14)(.672 \times 10^{-4})^2}$$

$$= 174{,}000 \text{ psi.}$$

$$\tau_{\substack{max.\ limiting \\ typical}} = .31\ q_{o\ lim.} = (.31)(174{,}000)$$

$$= 53{,}900 \text{ psi.}$$

The smallest radius R_2, and therefore the largest q_o limiting for a given load and R_1 is $R_2 = .0012$ in. This corresponds to a ratio of $\frac{.0040}{.0012} = 3.33$ which is just outside the limiting range of 2.5 to 3. Using this value of R_2 gives:

$$\frac{1}{R_o} = \frac{1}{R_1} + \frac{1}{R_2} = \frac{1}{.0012} + \frac{1}{-.0040} = 583 = \frac{1}{.001718}$$

$$a = (.672 \times 10^{-4})\left[\frac{.001718}{.00240}\right]^{1/3} = (.672 \times 10^{-4})(.8945)$$

$$= .0000595$$

$$q_{o\ \substack{limiting \\ extreme}} = \frac{174{,}000}{(.8945)^2} = \frac{174{,}000}{.8} = 217{,}000 \text{ psi.}$$

Thus $q_{o\ limiting} \approx 200{,}000$ psi. is reasonable for glass with a hardened steel pivot.

For a Sapphire Jewel

$$\frac{1}{R_o} = \frac{1}{R_1} + \frac{1}{R_2} = \frac{1}{.0035} + \frac{1}{-.0100} = 186 = \frac{1}{.00537}$$

$$\frac{1}{E_o} = (1 - \nu^2)\left[\frac{1}{E_1} + \frac{1}{E_2}\right] = (1 - .3^2)$$

$$\left[\frac{1}{30 \times 10^6} + \frac{1}{52.5 \times 10^6}\right]$$

$$= \frac{.91}{19.11 \times 10^6} = \frac{1}{21 \times 10^6}$$

In this case we take $q_{o\ limiting}$ as known (at something slightly less than 300,000 psi: say 285,000 psi.) and solve Equations 132 and 133 for P.

$$(137) \qquad P_{limiting} = \frac{\left[\frac{3}{4}\frac{R_o}{E_o}\right]^2}{\left[\frac{3}{2\pi\, q_{o\ limiting}}\right]^3}$$

$$= \frac{\left[\frac{(3)(.00537)}{(4)(21 \times 10^6)}\right]^2}{\left[\frac{(3)}{(2)(3.14)(285{,}000)}\right]^3} = \frac{\left[1.92 \times 10^{-10}\right]^2}{\left[1.675 \times 10^{-6}\right]^3}$$

$$= \frac{3.68 \times 10^{-20}}{4.7 \times 10^{-18}} = .00784 \text{ lb.}$$

$$a = \left(\frac{3P\ R_o}{4E_o}\right)^{1/3} = \left[\frac{(3)(.00784)(.00537)}{(4)(2.\ \times 10^6)}\right]^{1/3}$$

$$= \left[1.502 \times 10^{-12}\right]^{1/3}$$

$$= .0001145 \text{ in.}$$

$$\frac{a}{R_2} = \frac{1.145}{35} = .0327 \text{ (which is small enough)}$$

$$\alpha = \frac{a^2}{R_o} = \frac{(1.145 \times 10^{-4})^2}{5.37 \times 10^{-3}} = 2.44 \times 10^{-6} \text{ in.}$$

As a check,

$$q_o = \frac{3P}{2\pi a^2} = \frac{(1.5)(.00784)}{(3.14)(1.145 \times 10^{-4})^2} = 285{,}000 \text{ psi.}$$

Thus for a limiting sapphire jewel pressure, q_o limiting = 285,000 psi. and for the standard bearing with the largest radius of curvature (minimum stress for a given load) the ratio

$$\frac{p_{\text{limiting sapphire}}}{p_{\text{limiting glass}}} = \frac{.00784}{.00165} = 4.75$$

Estimation of Loads on the Bearings

In order to calculate the loads on the bearing in the projectile it is necessary to know the maximum axial and radial accelerations of the pivoted mass.

Let:

$\bar{a}$ = axial acceleration of c.g. of shell (in./sec^2)

ω = ang. vel. of shell about its axis (rad./sec.)

ℓ = lead of rifling (in./rev.)

F = gas force on shell, average (lbs.)

A = area that gas pressure acts upon (in.^{2})

P = gas pressure, average (psi.)

W = weight of shell (lbs.)

I = moment of inertia of shell about its axis (lbs. sec^2 in.)

r = outside radius of shell (in.)

b = radial distance from centerline of shell to centerline of a shaft in the mechanism (in.)

g = acceleration of gravity (in./sec.^{2})

L = length of barrel (in.)

$\bar{v}$ = axial velocity of center of gravity of shell (in./sec.)

a_{radial} = radial acceleration at the centerline of pivoted shaft (in./sec.^{2})

Use the following as typical data:

W = 35 lb.

P = 17,000 psi. (assumed constant)

r = 3 in.

ℓ = 120 in./1.5 rev. = 80 in./rev.

L = 120 in.

b = .375 in.

Then

$$A = \pi r^2 = (3.14)(3)^2 = 28.3 \text{ in.}^2$$

To calculate the shell moment of inertia assume that all its mass is concentrated at a distance k = 2.5 in. from the shell centerline. Then

$$I = \frac{W}{g} k^2$$

Equating the work done on the shell in time dt to its change in kinetic energy (assuming that losses are taken care of by the choice of P) gives

$$PA\bar{v}dt = \frac{1}{2}\frac{W}{g}\left[(\bar{v} + d\bar{v})^2 - (\bar{v})^2\right] + \frac{1}{2}\left(\frac{W}{g}k^2\right)\left[(\omega + d\omega)^2 - \omega^2\right]$$

$$= \frac{W}{g}\left[\bar{v}d\bar{v} + k^2\,\omega\,d\omega\right]$$

But

$$\omega = \bar{v}\frac{2\pi}{\ell} \text{ and } d\omega = \frac{2\pi}{\ell}d\bar{v}$$

so that

$$PAdt = \frac{W}{g}\left[d\bar{v} + k^2\left(\frac{2\pi}{\ell}\right)^2 d\bar{v}\right]$$

or since $\bar{a} = \frac{d\bar{v}}{dt}$

(138) $$\frac{a_{axial\ av}}{g} = \frac{PA}{W\left[1 + \frac{k^2 (2\pi)^2}{\ell^2}\right]}$$

The maximum velocity (muzzle velocity) is

(139) $$\bar{v}_{max.} = (2\bar{a}L)^{1/2}$$

and the maximum angular velocity (the spin speed during flight) is

(140) $$\omega_{max.} = \bar{v}_{max.}\left(\frac{2\pi}{\ell}\right)$$

The radial acceleration of the pivoted mass during flight is then

(141) $$a_{rad.} = (\omega_{max.})^2\, b$$

Using the assumed typical values gives

$$\frac{\bar{a}_{axial}}{g} = \frac{PA}{W\left[1 + \frac{k^2 4\pi^2}{\ell^2}\right]} = \frac{(17,000)(28.3)}{(35)\left[1 + \frac{2.5^2 (6.28)^2}{80^2}\right]}$$

$$= 13,300$$

and

$$\bar{v}_{max.} = (2\bar{a}\ L)^{1/2} = ((2)(13,300 \times 386)(120))^{1/2}$$

$$= 35,300 \text{ in./sec.}$$

$$= 2,920 \text{ ft./sec.}$$

which seems reasonable as a muzzle velocity.

$$\omega_{max.} = \bar{v}_{max.} \frac{2r}{l} = (35,100)\ \frac{6.28}{80} = 2,760 \text{ rad./sec.}$$

$$a_{radial} = (\omega_{max.}{}^2) b = (2,760)^2\ (.375) = 2.85 \times 10^6 \text{ in./sec.}^2$$

$$\frac{a_{radial}}{g} = \frac{2,850,000}{386} = 7,400$$

In order to calculate the pivoted weight assume that a typical gear has:

O.D. = .383 in. = D

Thickness = .0242 in. = t

Wt. Density = .3 lb./in.^{3} = γ

Then the gear weight = (γ) (volume) = (.3)(.785 x .383^2)(.0242)

Typ. gear wt. = .000835 lb.

For the heaviest gear use:

$$O.D. = .4496 \text{ in.}$$

$$t = .0515 \text{ in.}$$

$$\gamma = .3 \text{ lb./in.}^3$$

$$\text{Heaviest gear weight} = (.000835)\left[\frac{.0515}{.0242}\right]\left[\frac{.4496}{.383}\right]^2 = .00245 \text{ lb.}$$

Allowing for pinion and shaft weight gives:

$$W_{\text{pivoted typ.}} \approx .0012 \text{ lb.} \quad \text{(say)}$$

$$W_{\text{pivoted max.}} \approx .0030 \text{ lb.} \quad \text{(say)}$$

The axial load P applied to the aft.- bearing is then

(142) $$P_{\text{typ.}} = W_{\text{typ.}} \frac{\bar{a}}{g} = (.0012)(13,300) = 15.95 \text{ lb.}$$

or

$$P_{\text{max.}} = W_{\text{max.}} \frac{\bar{a}}{g} = (.0030)(13,300) = 39.9 \text{ lb.}$$

From Equation 132 (for a fixed R_o and E_o or equivalentlly for a given bearing)

(143) $$a' = \left(\frac{P'}{P}\right)^{1/3} a$$

where primes denote loads and dimensions in the projectile and no primes denote these quantities in typical insturments with limiting loads.

Similarly from Equation 137 (for a fixed R_o and E_o)

(144) $$q_o' = q_o \left[\frac{P'}{P} \right]^{1/3}$$

Since

$$\left[\frac{P'_{typ.}}{P} \right]^{1/3} = \left(\frac{15.95}{.00784} \right)^{1/3} = (2,035)^{1/3} = 12.68$$

(P = .00784 lb. for sapphire bearing with the highest rating)

the maximum contact pressure in the bearing would be

$$q'_{o\ typ.} = q_o \left(\frac{P'}{P} \right)^{1/3} = (285,000)\ (12.68)$$

$$= 3,610,000 \text{ psi.}$$

(See P. 108 for q_o)

which of c urse is excessive.

B. Required Size of a Vee Jewel Bearing That Can Withstand The Axial Acceleration.

From SECTION IV A, P. 101 we have

(130) $$\frac{1}{R_o} = \frac{1}{R_1} + \frac{1}{R_2}$$

(131) $$\frac{1}{E_o} = \frac{1 - \nu_1^2}{E_1} + \frac{1 - \nu_2^2}{E_2}$$

(132) $$a^3 = \frac{3}{4}\frac{P\,R_o}{E_o}$$

(133) $$q_o = \frac{3P}{2\pi a^2}$$

In these equations we can regard the materials and load as given and then solve for the required sizes.

Using the strongest combination (sapphire and hard steel) we have

$$\frac{1}{E_o} = \frac{1}{21 \times 10^6}$$ (Page 108)

$q_{o\ limiting} = 285{,}000$ psi. (Page 108)

$P_{typical} = 15.95$ lb., $P_{max.} = 39.9$ lb. (Page 114)

Taking the ratio of $|R_1|$ to $|R_2|$ as (Page 105)

$$\left|\frac{R_1}{R_2}\right| = \frac{.0100}{.0035} = 2.86$$

gives for R_o

(145) $$R_o = \frac{R_1 R_2}{R_1 + R_2} = R_1 \frac{1}{1 + \frac{R_1}{R_2}}$$

$$= R_1 \frac{1}{1 + \frac{-.0100}{.0035}} = -.538 R_1$$

Eliminating a between 132 and 133 and solving for R_o gives

(146) $$R_o = \left(\frac{4}{3}\right) \left(\frac{3}{2\pi}\right)^{3/2} \frac{P^{1/2} E_o}{q_o^{3/2}}$$

or (using 145)

(147) $$R_1 = \left(\frac{4}{3}\right) \left(\frac{3}{2\pi}\right)^{3/2} \frac{P^{1/2} E_o}{q_o^{3/2}} \left(1 + \frac{R_1}{R_2}\right)$$

(147) $$R_1 = \frac{.44\ P^{1/2}\ E_o}{q_o^{3/2}} \left(1 + \frac{R_1}{R_2} \right)$$

Using the numerical values above

$$R_{1\ \text{typical}} = \frac{(.44)(15.95)^{1/2}\ (21 \times 10^6)(1 - 2.86)}{(.285 \times 10^6)^{3/2}}$$

$$= -\ .452 \text{ in.}$$

As a check

$$R_{1\ \text{typ.}}' = R_1 \left[\frac{P'}{P} \right]^{1/2} = (-.010) \left[\frac{15.95}{.00784} \right]^{1/2} = -\ .452 \text{ in.}$$

where P = .00784 lb. for the sapphire bearing with the highest rated load.

$$R_{1\ \text{max.}} = (-.010) \left[\frac{39.9}{.00784} \right]^{1/2} = -\ .714 \text{ in.}$$

$$R_{o\ \text{typ.}} = -\ R_{1\ \text{typ.}}\ (.538) = (.452)(.538) = .243 \text{ in.}$$

$$R_{o\ \text{max.}} = -\ R_{1\ \text{max.}}\ (.538) = (.714)(.538) = .384 \text{ in.}$$

$$R_{2\ typ.} = \frac{R_{1\ typ.}}{2.86} = \frac{.452}{2.86} = .158 \text{ in.}$$

$$R_{2\ max.} = \frac{R_{1\ max.}}{2.86} = \frac{.714}{2.86} = .250 \text{ in.}$$

$$a_{typ.} = \left(\frac{3}{4}\,\frac{P\ R_o}{E_o}\right)^{1/3} = \left(\frac{3}{4} \times \frac{15.95 \times .243}{21 \times 10^6}\right)^{1/3}$$

$$= (.1381 \times 10^6)^{1/3}$$

$$= .00517 \text{ in.}$$

$$\frac{a_{typ.}}{R_{2\ typ.}} = \frac{.00517}{.158} = .0328$$ (See P. 109 for a check)

which is small enough.

As a check and in order to see how a varies we have from Equation 133 (keeping q_o fixed by adjusting R_o)

$$a'_{typ.} = \left(\frac{P'\ typ.}{P}\right)^{1/2} a = \left(\frac{15.95}{.00784}\right)^{1/2} (.0001145)$$

(148) $$= (45.2)(.0001145)$$

$$= .00515 \text{ in.}$$

C. **Friction Torque Developed on a Vee Jewel Bearing That is Required to Allow Rotation During the Axial Acceleration Period**

Neglect the effects of the transverse loading for simplicity since it is due primarily to $\omega^2 b$ rather than αb ($\alpha = \frac{d\omega}{dt}$)(see P. 113). The transverse loading becomes significant near the end of the axial acceleration period and remains significant during flight. It is therefore treated separately.

The deformed surfaces are essentially plane with a hemispherical pressure distribution given by

$$q(r) = q_o \left[1 - \frac{r^2}{a^2}\right]^{1/2} \tag{149}$$

where:

r is the variable radius (in.)

a is the outside radius of the contact circle (in.)

q_o is the contact pressure at the center (psi) and

q is the contact pressure at radius r (psi).

Letting

μ = coefficient of friction

dT_{fr} = friction torque on an annulus of radius r and thickness dr (in. lb.)

and

$$T_{fr} = \text{Total friction torque (in.lb.)}$$

we have

$$dT_{fr} = \mu\, q(r)(2\pi r\, dr)(r) = 2\pi\mu q_o \left[1 - \frac{r^2}{a^2} \right]^{1/2} r^2 dr$$

Integrating from $r = 0$ to $r = a$ gives

$$T_{fr} = 2\pi\mu q_o\, a^3 \int_{\frac{r}{a}=0}^{\frac{r}{a}=1} \left[1 - \frac{r^2}{a^2}\right]^{1/2} \frac{r^2}{a^2}\, d\left(\frac{r}{a}\right)$$ (See Pierce #145, P.21)

(150) $$T_{fr} = \mu q_o\, a^3 \frac{\pi^2}{8}$$

Using Eq. 133 to eliminate a gives

(151) $$T_{fr} = \left(\frac{1}{8}\right)\left(\frac{3}{2}\right)^{3/2} (\pi)^{1/2}\ \mu \frac{P^{3/2}}{q_o^{\ 1/2}}$$

Thus if the bearing must rotate while axial acceleration is occurring, the friction torque goes up as the $\frac{3}{2}$ power of axial load P for a fixed design q_o.

For the largest radius standard sapphire bearing under its limiting load we have (P. 108)

$$P = .00784 \text{ lb.}$$

and

$$q_o = 285{,}000 \text{ psi.}$$

Taking $\mu = .17$ (half way between .15 and .19 listed as typical in the Richard H. Bird catalog) gives

$$T_{\substack{\text{fr. largest} \\ \text{std. brg.} \\ \text{under its maximum load}}} = \left(\frac{1}{8}\right)\left(\frac{3}{2}\right)^{3/2} (\pi)^{1/2} \frac{\mu P^{3/2}}{q_o^{1/2}}$$

$$= (.407)(.17)\frac{(.00784)^{3/2}}{(285{,}000)^{1/2}}$$

$$= (.0692)\frac{(.000694)}{(534)}$$

$$= 8.98 \times 10^{-8} \text{ in. lb.}$$

As a check

$$a^3 = 1.502 \times 10^{-12} \text{ (P. 109)}$$

Equation 149 gives

$$T_{fr} = \mu q_o \, a^3 \, \frac{\pi^2}{8} = (.17)(285{,}000)(1.502 \times 10^{-12}) \, \frac{3.14^2}{8}$$

$$= 8.96 \times 10^{-8} \text{ in.lb.}$$

If the load is increased to $P_{typ.} = 15.95$ lb

$$T_{fr.\ \text{bearing reqd. to withstand acc. (typical wt. shaft)}} = T_{fr\ \text{largest std. brg.}} \left(\frac{P'_{typ.}}{P}\right)^{3/2}$$

with q_o kept constant. This gives

$$T'_{fr.\ typ.} = (8.98 \times 10^{-8})\left(\frac{15.95}{.00784}\right)^{3/2}$$

$$= (8.98 \times 10^{-8})(9.19 \times 10^{4})$$

$$= .00825 \text{ in. lb.}$$

for the typical shaft and

$$T'_{fr.\ max.} = (8.98 \times 10^{-8})\left(\frac{39.9}{.00784}\right)^{3/2}$$

$$= (8.98 \times 10^{-8})(36.35 \times 10^{4})$$

$$T'_{fr.\ max.} = .0327 \text{ in. lb.}$$

for the heaviest shaft. In order to decide whether these torques are acceptable or excessive, we perform the following rough calculations.

The shafts are driven from the mainspring shaft through pinions on the shafts. Using a pinion radius $r_{p\ typ.} = .058$ in. and $r_{p\ heaviest\ shaft} = .106$ gives as the tangential force required to overcome only its own aft bearing friction:

$$F_{tan.\ typical} = \frac{T_{fr.\ typ.}}{r_{p\ typ.}} = \frac{.00825}{.058} = .142 \text{ lb.}$$

and

$$F_{tan.heaviest} = \frac{T_{fr.\ heaviest}}{r_{p\ heaviest}} = \frac{.0327}{.106} = .309 \text{ lb.}$$

These forces may be compared to the total transverse force acting on the shaft due to spin of the projectile:

$$F_{\substack{transverse\\ inertia\\ typ.\ max.}} = W_{typ.} \frac{a_{rad.\ max.}}{g} = (.0012)(7,400) = 8.87 \text{ lb.}$$

and

$$F_{\substack{\text{transverse}\\ \text{inertia}\\ \text{heaviest max.}}} = (W_{\text{heaviest}}) \frac{a_{\text{rad. max.}}}{g} = (.0030)(7,400)$$

$$= 22.2 \text{ lb.}$$ (See Pages 113 and 114 for these values.)

Therefore these friction torques are not excessive in the sense that they will cause excessive bending stresses in the shafts, since the bending effect due to the friction torques is so much less than that due to the transverse inertia forces.

Before accepting the possibility of rotation in a bearing during the axial acceleration period we should consider that a, the radius of the contact circle, is 45.2 (see P. 119) times as large here as for the largest standard bearing. Thus for the same angular speeds, the rubbing velocities are 45.2 times as large. This may not be acceptable.

So consider the situation from the point of view of required mainspring energy. The time t (sec.) that the projectile spends under acceleration (in the barrel) is (see PP. 110 and 112)

$$t = \left[\frac{2L}{\bar{a}_{\text{av. axial}}} \right]^{1/2} = \left[\frac{(2)\ (120)}{(386)(13,300)} \right]^{1/2} = .00683 \text{ sec.}$$

If the shaft is rotating at n rpm it makes $\frac{nt}{60}$ revolutions while under axial acceleration. The frictional energy lost is then

$$E_{friction} = (T_{fr}) \left(\frac{nt}{60}\right) \text{ in. lb. per shaft.}$$

Assuming a steel mainspring with 50% energy storage efficiency and a maximum design tensile stress of 180,000 psi. gives as the energy per unit volume

$$U/vol. = (.50)(1/2)\frac{S_{max.}^2}{E} = (.25)\frac{(180,000)^2}{30 \times 10^6}$$

$$= 270 \text{ in. lb/in.}^3$$

Assuming a mainspring volume of 80% of a cylinder ¼ inch long and 1.4 inches outside diameter gives as the available stored energy

$$U_{stored} = \left(\frac{U}{vol.}\right)(.8)(.25)(.785)(1.4)^2$$

$$= (270)(.308) = 83 \text{ in. lb.}$$

The energy lost in a shaft of typical weight is

$$E_{fr.\ typ.} = T_{fr.}\ \frac{nt}{60} = \frac{(.00825)\ n\ (.00683)}{60}$$

$$= .94 \times 10^6 \times n \text{ in. lb. per typ. shaft}$$

(See Pages 123 and 125 for these values.)

Assuming a speed of 20 rpm for the fastest typical weight shaft gives

$$E_{\substack{fr.\ fastest\ typ.\\ wt.\ shaft}} = .94 \times 10^{6} \times 20 = .0000188 \text{ in. lb.}$$

Clearly then energy loss during the initial acceleration period is no problem.

However, the product of muzzle velocity (2920 f.p.s.) (P. 113) and barrel time (.00583 sec.)(P.125) is 20 ft. (two barrel lengths). This represents a maximum error in range if we have assumed that the timer started when firing was initiated and it actually starts when the shell leaves the barrel. Thus while the calculations above indicate that a bearing that can withstand the axial acceleration loads can also allow rotation during the axial acceleration period, as a practical matter this may not be desirable.

<u>Friction Radius of Vee Jewel Bearing</u>

Since

$$(150) \qquad T_{fr} = \mu q_o \, a^3 \, \frac{\pi^2}{8}$$

and the normal force is

$$(133) \qquad P = \frac{2\pi \, q_o \, a^2}{3}$$

if we define the friction radius r_{fr} (in.) by

(153) $$r_{fr} = \frac{T_{fr}}{\mu P}$$

we have

(154) $$r_{fr} = \frac{3\pi}{16} a = .588\ a = .294\ (2a)$$

for this hemispherical pressure distribution. For

$$a = .00516 \text{ in. (P.119)}$$

$$r_{fr} = .588\ (.00516) = .00304 \text{ in.}$$

which is extremely small for a shaft and bearing subjected to an axial load of 15.95 lb.

D. <u>Effect of Transverse Load Upon a Vee Jewel Bearing</u>

Consider the enlarged view of the vee bearing shown in Figure 22. Assume that the bearing is exerting a force on the shaft that supplies all the axial acceleration and half of the transverse acceleration. From PP. 112 and 113

$$\frac{\bar{a}_{axial}}{g} = 13,300$$

$$\left(\frac{1}{2}\right)\left(\frac{a_{rad.\ max.}}{g}\right) = \left(\frac{1}{2}\right)(7,400) = 3,700$$

Thus the resultant force makes an angle α with the shaft centerline given by (Fig. 23)

$$\alpha = \tan^{-1}\frac{\frac{1}{2}\,a_{rad.\ max.}}{\bar{a}_{axial}} = \tan^{-1}\frac{3,700}{13,300} = 15.53^{\circ}$$

Assuming temporarily that the forward bearing only applies a transverse restraint to the shaft, and that the resultant force exerted by the aft bearing remains normal to the bearing surface gives the geometric picture shown in Figure 24. The pivot rises and remains parallel to its original position so that contact occurs at the angle α to the shaft center-line. In terms of R_1 and R_2 (P.99) we can calculate the offset e(in.) and the rise r (in.)

FIGURE XXII

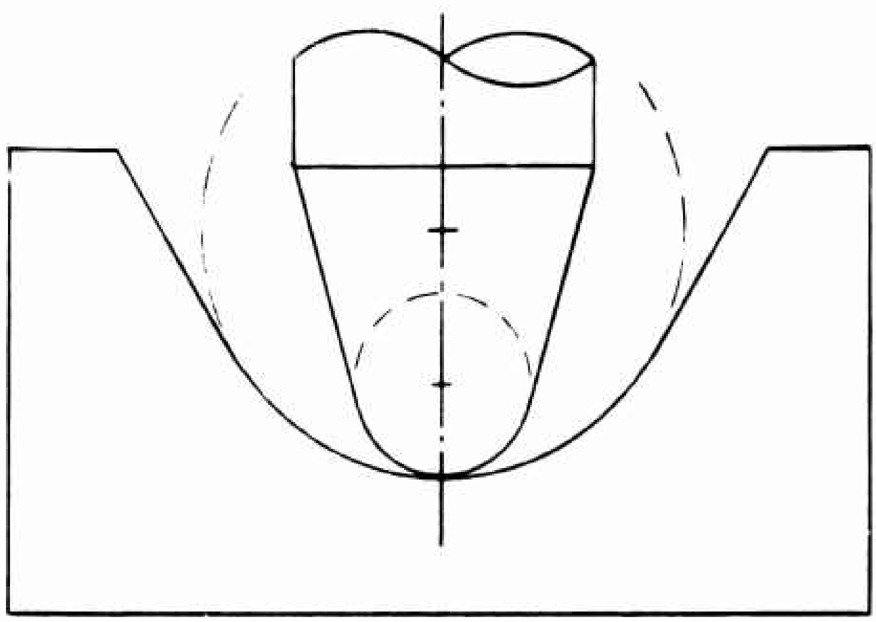

VEE JEWEL BEARING

FIGURE XXIII

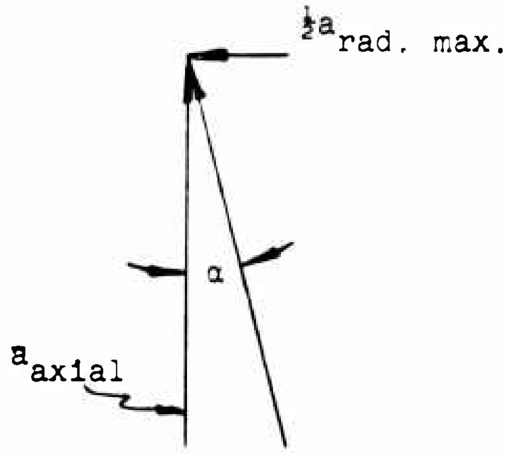

ACCELERATION VECTORS

FIGURE XXIV

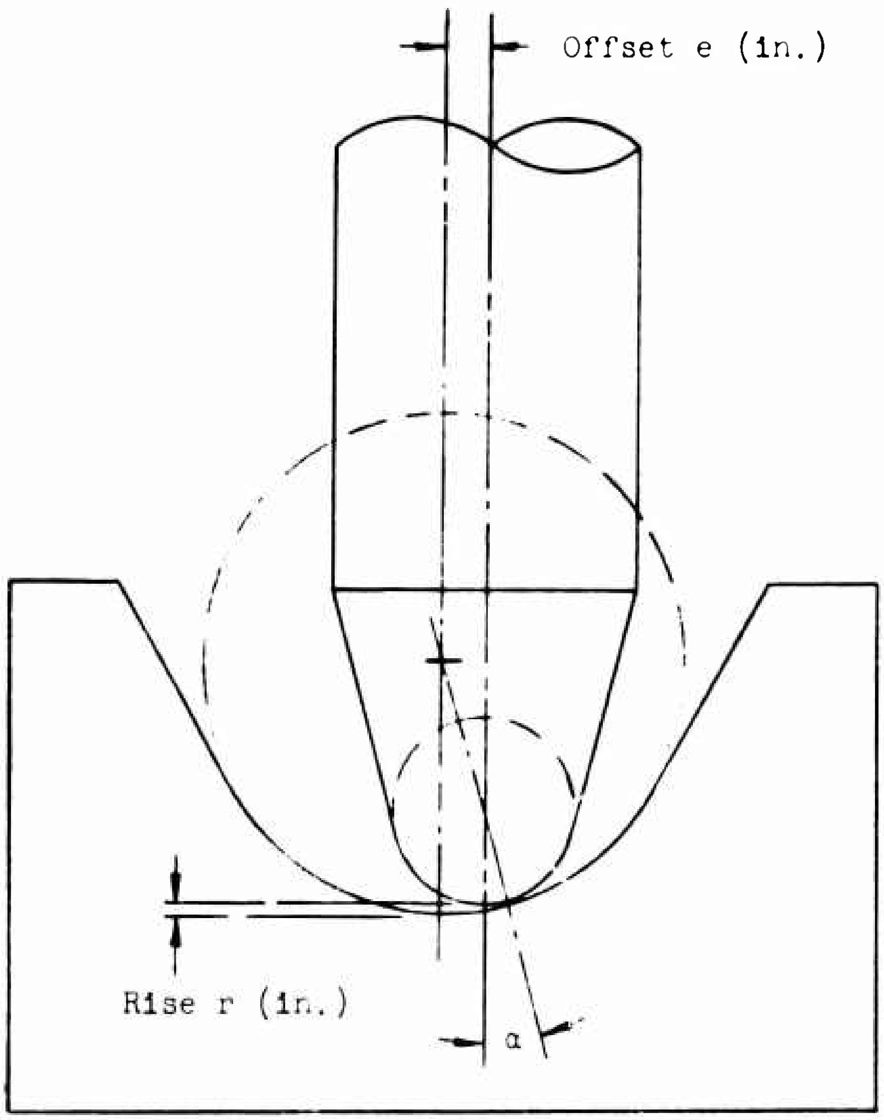

VEE JEWEL BEARING SHOWING OFFSET

DUE TO RADIAL ACCELERATION

$$e = (|R_1| - |R_2|) \sin\alpha$$

$$r = (|R_1| - |R_2|)(1 - \cos\alpha)$$

Numerically we have (see PP. 118 and 119)

$$e = (|R_1| - |R_2|) \sin\alpha = (.452 - .158)(1 - \cos 15.53^\circ)$$

$$= .0798 \text{ in.}$$

$$r = (|R_1| - |R_2|)(1 - \cos\alpha)$$
$$= (.452 - .158)(1 - \cos 15.53^\circ)$$
$$= .01076 \text{ in.}$$

Since these are both excessive, consider the helping effect of friction, which was ignored in the above calculations. Coefficients of pivoting friction are given in the R. H. Bird catalog as varying between .15 and .19. When we are relying on the friction to help withstand the transverse load it is reasonable to use $\mu = .12$ as a conservative design value. The corresponding angle of friction ϕ is then

$$\phi = \tan^{-1} \mu = \tan^{-1} .12 = 6.85^\circ$$

and the resultant force would act 6.85° from the normal to the contact surfaces. Since the resultant force must act at an angle $\alpha = 15.53^\circ$ to the shaft centerline, the contact angle with friction, α_{fr}, is given by

$$\alpha_{fr} = \alpha - \phi = 15.53^\circ - 6.85^\circ = 8.68^\circ$$

and

$$e = (|R_1| - |R_2|) \sin\alpha_{fr} = (.452 - .158)(\sin 8.68^\circ)$$

$$= .0443 \text{ in.}$$

$$r = (|R_1| - |R_2|)(1 - \cos\alpha_{fr})$$

$$= (.452 - .158)(1 - \cos 8.68^\circ)$$

$$= .00335 \text{ in.}$$

This offset is still completely unacceptable. It has been computed using the large axial load of the initial acceleration period and the transverse load that exists during flight. It should be noted however, that as the axial load decreases the offset increases still more.

E. <u>Summary of Conclusions About the Suitability of Vee Jewel Bearings</u>

The axial load required to accelerate the mass carried by a typical shaft of this mechanism is about 15.95 lb. (P. 114) while the strongest vee jewel bearing typical of standard commercial practice can operate under a load of only .00784 lb. (P. 108). Since the required radius of curvature increases with the square root of the axial load for fixed elastic properties, radius ratio, and limiting stress (see Equation 147), this means that the jewel radius of curvature must increase by a factor of 45.2 to become .452 in. (P. 118). The radius of the contact circle also increases with the square root of the load (P.119) and becomes .00516 in. on the typical shaft.

Vee jewel bearings with these increased radii and associated dimensions are not presently made commercially. It does not appear that there is any severe technological limit associated with this increased size, but rather that there is no present commercial demand for such bearings. Aside from greatly increased cost the only design limit that the writer can see associated with the larger bearings is to require a somewhat lower (say 15%) design maximum compressive stress to account for the greater chance of imperfections and the effects of higher rubbing speeds in the larger bearings.

The friction torque of these larger bearings, even while operating under maximum axial load, is still very small, primarily because the radius of the contact circle is only .00516 in. (P. 119) and the effective friction radius is then only .00304 in. (P. 128).

The severe limitation on the use of the vee jewel bearing in the present application is the presence of relatively high transverse loads of approximately 4.43 lb. per bearing (P. 124) during the time of operation due to the spin of the projectile, and the necessary offset of at least some shaft from the projectile axis. An excessive shaft offset under load is required to change the direction of the normal to the contact surfaces from its original direction parallel to the shaft axis to a direction with a component transverse to the shaft. Thus, neglecting friction, and favorably assuming that the initial high axial force remains, we get a calculated offset of .0798 in. (P. 132), while considering both friction and the favorable effect of high axial force, only reduces the calculated offset to .0443 in. (P. 133). Both of these values are excessive in the precision type mechanism under consideration, and both would have to be increased to account for the reduction in axial load after the initial acceleration period.

Thus to summarize, vee type bearings could probably be made to withstand the axial loads and to give low friction in operation, but have to be rejected because they cannot apply sufficient transverse constraint to the pivoted parts.

SUMMARY AND CONCLUSIONS

In this section the results and conclusions of the investigation are summarized and briefly discussed. More complete discussions are given in the body of the report.

In the first part of Section I, formulas are developed for sizing bearings which have combined axial and transverse load capacity when axial load controls sizing. Ten cases are considered as follows:

Case I Flat bearing-uniform normal pressure distribution. (This bearing has no transverse load capacity but is included since its axial load capacity serves as a convenient reference value and since it can be used in conjunction with a journal bearing.)

Case II Flat bearings with linear normal pressure distributions.

Case III Full spherical bearings with a uniform normal pressure distribution.

Case IV Hollow spherical bearings with a uniform normal pressure distribution.

Case V Full spherical bearing with a cosine normal pressure distribution.

Case VI Hollow spherical bearing with a cosine normal pressure distribution.

Case VII (Hollow) torroidal bearing with a uniform normal pressure distribution.

Case VIII (Hollow) torroidal bearing with a cosine normal pressure distribution.

Case IX Hollow conical bearing with a uniform normal pressure distribution.

Case X Bearing with theoretical line contact along a circle of latitude.

In each of these cases an expression is derived giving the dimensionless outside radius ratio (the ratio of the required outside radius to a reference outside radius as determined by axial load) as a function of the dimensionless geometric parameters that describe the bearing and the dimensionless parameters that fix the loading.

As would be expected, the smallest required size for any shape occurs when the inner radius is zero, and the required size increases with increasing inner radius. In addition a uniform pressure distribution gives the smallest required size, irrespective of shape. The more realistic pressure distributions, which drop off with increasing rddius, require a larger size and do depend upon bearing shape. Thus for example we see that the shallow spherical bearing (α small, see P. 10, Fig. 5) requires a smaller size, under axial load, than its deeper (α large) counterpart. Figure 5 also shows that the deep hollow spherical bearing with α between 60° and 90°, and with a (reasonable) cosine pressure distribution, requires about the same size as a flat bearing with a (reasonable) trapezoidal load distribution ($\eta = .5$). Since the deep spherical bearing has transverse load capacity and the flat bearing does not, their similarity in axial load size for realistic load distributions is a strong point in favor of the deep spherical bearing. An additional result of interest is that the deep torpoidal bearing with $\alpha = 90^{\circ}$ requires a larger size than the deep hemispherical bearing with $\alpha = 90^{\circ}$.

Another interesting result is that with theoretical line contact (Case 10) the required size of bearing is only about three times that of a bearing of similar materials and design stresses but with theoretical area contact. This indicates that further careful consideration of bearings with theoretical line contact is warranted.

In the second part of Section I, equations for the friction torque and the dimensionless friction radius ratio are developed for the 10 cases of the first part when the bearings are operating under axial load alone. Since this operation occurs over such a short interval, if it is required at all, the choice of bearing shapes or parameters would not be influenced very much by the requirement of low friction torque under axial load. However, the order of magnitude of friction torques in these cases is of interest, and they are not excessive.

In Section II the bearings of the first section are analyzed when they are operating under transverse load. Because the flat bearings cannot take any transverse load, and because one normal pressure distribution was much more reasonable than most others there are only four distinct cases. They are: spherical bearings (hollow and solid), torroidal bearings, conical bearings and bearings with latitude circle line contact. In each of these cases formulas for the dimensionless bearing size as determined by transverse load capacity and for the dimensionless friction radius ratio under transverse load are derived. Numerical values are calculated and it is found that with the load magnitudes used, either axial or transverse load capacity may determine the required bearing size. The one that controls depends upon the particuaar type of bearing and the value of its geometric parameters. This approximate balance of the size requirements is good in that the axial load does not demand increased size which will give increased friction when the bearing is operating under transverse load.

Another result of interest is that the deep spherical bearings ($\alpha = 90^{\circ}$) have less friction torque than shallow ones ($\alpha = 30^{\circ}$) of the same transverse load capacity and radius ratio β (see PP. 66 and 67). In addition the spherical bearings have somewhat less friction than the torroidal bearings of the same angle α and radius ratio β (see P. 74). The conical bearing (P. 75) and the line contact bearing (P. 78) also have reasonable typical sizes and friction torque under transverse load and furthur consideration of both of these bearings is warranted.

In Section III methods of analyzing journal bearings for contact stresses and friction torque in terms of load are developed and some numerical results are obtained. The two conclusions of interest are that these bearings are feasible and that a simple support will create less friction than a restrained support.

In Section IV methods of computing contact stresses and friction torques for a vee bearing are presented. It may be noted that since the theory applies to a spherical shaft end in a larger radius spherical socket, a separate ball may be used to replace the shaft end. Design equations are developed for sizing these bearings under axial load and these equations are applied to jewel bearings. The feasibility of using standard jewel bearings under the axial acceleration loads is also investigated and it is found that bearings much larger than those that are presently made commercially are necessary. It is also found that these bearings cannot withstand the high transverse loads. Expressions for the friction torque are also developed for these bearings under axial load.

DISTRIBUTION

2 - Commanding General
U. S. Army Materiel Command
Attn: AMCRD-DE-W
AMCPM-SW
Washington, D. C. 20315

3 - Commanding General
U. S. Army Munitions Command
Attn: AMSMU-RE-EM
Dover, New Jersey -7801

2 - Commanding Officer
Picatinny Arsenal
Attn: SMUPA-Technical Library
Dover, New Jersey 07801

1 - Headquarters
U. S. Continental Army Command
Fort Monroe, Virginia

1 - Commanding General
U. S. Army Test & Evaluation Command
Attn: Technical Library
Aberdeen Proving Ground
Maryland 21005

1 - Commanding Officer
Harry Diamond Laboratories
Connecticut Avenue &
Van Ness Street, N. W.
Attn: Technical Reference Section
Washington, D. C. 20438

11- Commanding General
U. S. Army Missile Command
Redstone Arsenal
Attn: Technical Library
Huntsville, Alabama 35809

1 - Commanding Officer
U. S. Army Ballistics Research Labs
Aberdeen Proving Ground
Maryland 21005

1 - Director
Advanced Research Projects Agency
Attn: Col. B. H. Elliott, USMC
Washington 25, D. C.

20 - Defense Documentation Center
Cameron Station
Alexandria, Virginia 22314

4 - Commanding Officer
Frankford Arsenal
Philadelphia, Pa. 19137
Attn: SMUFA 1610
O. Ehrman